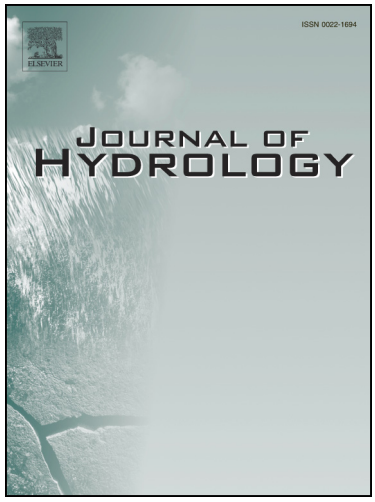

Application of isotopic tracers as a tool for understanding hydrodynamic behavior of the highly exploited Diass aquifer system (Senegal)

Diakher Hélène Madiounea, Serigne Faye, Philippe Orban, Serge Brouyère, Alain Dassargues, Jacques Mudry, Christine Stumpp, Piotr Maloszewski

PII: S0022-1694(14)00059-6
DOI: http://dx.doi.org/10.1016/j.jhydrol.2014.01.037
Reference: HYDROL 19353

To appear in: *Journal of Hydrology*

Received Date: 6 May 2013
Revised Date: 7 January 2014
Accepted Date: 20 January 2014

Please cite this article as: Madiounea, D.H., Faye, S., Orban, P., Brouyère, S., Dassargues, A., Mudry, J., Stumpp, C., Maloszewski, P., Application of isotopic tracers as a tool for understanding hydrodynamic behavior of the highly exploited Diass aquifer system (Senegal), *Journal of Hydrology* (2014), doi: http://dx.doi.org/10.1016/j.jhydrol.2014.01.037

Application of isotopic tracers as a tool for understanding hydrodynamic behavior of the highly exploited Diass aquifer system (Senegal)

Madioune D.H. [1,2], Faye S.[1], Orban Ph.[2], Brouyère S.[2], Dassargues A.[2], Mudry J.[3], Stumpp C.[4], Maloszewski P.[4 @]

Diakher Hélène **Madioune** [1, 2]

[1] Department of Geology, Cheikh Anta DIOP University Dakar, Senegal

[2] Hydrogeology & Environmental Geology, Dpt ArGEnCo, Aquapole, University of Liege, Belgium

(E-mail: diakherm@yahoo.fr)

Serigne **Faye**

[1] Department of Geology, Cheikh Anta DIOP University Dakar, Senegal

(E-mail: serigne_faye@yahoo.com)

Philippe **Orban**

[2] Hydrogeology & Environmental Geology, Department ArGEnCo, Aquapole, University of Liege, Belgium

(E-mail: p.orban@ulg.ac.be)

Serge **Brouyère**

[2] Hydrogeology & Environmental Geology, Department ArGEnCo, Aquapole, University of Liege, Belgium

(E-mail: Serge.Brouyere@ulg.ac.be)

Alain **Dassargues**

[2] Hydrogeology & Environmental Geology, Department ArGEnCo, Aquapole, University of Liege, Belgium

(E-mail: Alain.Dassargues@ulg.ac.be)

Jacques **Mudry**

[3] Chrono-Environment UMR 6249, Université de Franche-Comté, Besançon, France

(E-mail: jacques.mudry@univ-fcomte.fr)

Christine **Stumpp**

[4] Institute of Groundwater Ecology, Helmholtz Zentrum München, German Research Centre for Environmental Health (GmbH), Ingolstaedter Landstrasse 1, D-85764 Neuherberg, Germany

(E-mail: christine.stumpp@helmholtz-muenchen.de)

[@] Corresponding author:

Piotr **Maloszewski**

[4] Institute of Groundwater Ecology, Helmholtz Zentrum München, German Research Centre for Environmental Health (GmbH), Ingolstaedter Landstrasse 1, D-85764 Neuherberg, Germany

Phone: + 49 89 31872583

Fax: + 49 89 31873361

E-mail: maloszewski@helmholtz-muenchen.de

Abstract: The Diass horst aquifer system located 50 km east of Dakar (Senegal) is exploited in two main aquifers covered by a sandy superficial aquifer: the confined/unconfined Palaeocene karstic limestone and the confined Maastrichtian sandstone aquifer underneath. This system has experienced intensive groundwater abstraction during the last 50 years to supply increasing water demand, agricultural and industrial needs. The high abstraction rate from 1989 to 2009 (about 109,000 m^3/d) has caused a continuous groundwater level decline (up to 30 m), a modification of the groundwater flow and salinization in parts of the aquifers. The objective of the study is to improve our understanding of the system functioning with regards to high pumping, identify the geochemical reactions that take place in the system, infer origin and timing of recharge by using mainly stable ($\delta^{18}O$, $\delta^{2}H$, ^{13}C) and radioactive (^{3}H and ^{14}C) isotopes.

Water types defined in the Piper diagram vary in order of abundance from Ca-HCO_3 (65%), Ca/Na-Cl (20%), Na-HCO_3 (3%) and Na-Cl (12%). Values of $\delta^{18}O$ and $\delta^{2}H$ for the superficial aquifer range between -5.8 and -4.2‰ and between -42 and -31‰, respectively. For the Palaeocene aquifer they range from -5.8 to -5.0‰ and from -38 to -31‰, respectively; values in the Maastrichtian aquifer are between -5.9 and -4.3‰ for $\delta^{18}O$ and -38 to -26‰ for $\delta^{2}H$. Plotted against the conventional $\delta^{18}O$ *vs* $\delta^{2}H$ diagram, data from the upper aquifer exhibit a dispersed distribution with respect to isotopic fractionation while those of the Palaeocene and Maastrichtian aquifers are aligned parallel and slightly below/or on the Global Meteoric Water Line (GMWL) evidencing ancient waters which had evaporated during infiltration.

The low tritium (generally <0.7 TU) and ^{14}C (0.7-57.2 pmc) contents indicate predominance of older water being recharged during the Pleistocene and Holocene periods. However, few boreholes which exhibit high tritium (1.2-4.3 TU) and ^{14}C (65.7-70.8 pmc) values indicate some mixture with recent water likely through faulting and vertical drainage from the upper to deeper aquifers as well as lateral flow along flow paths to the piezometric depressions created by pumping.

Keywords: Environmental isotopes, recharge, Palaeocene, Maastrichtian, Diass horst

1 Introduction

Each atmospheric precipitation event is unique as far as its deuterium and oxygen 18 content are concerned. As stable isotopes of the water molecule are nearly conservative, they preserve the signature of atmospheric condition and carry it to the subsurface. Therefore, they can help reveal the origin and age of groundwater. Stable isotopes oxygen-18 ($\delta^{18}O$) and deuterium ($\delta^{2}H$) as well as radioactive isotopes tritium (^{3}H) and carbon-14 (^{14}C) have been proven to be important tools in answering important mechanisms in hydrogeology such as the origin of water, recharge and mixing processes, flow regime, residence time and changes in climatic conditions (Clark & Fritz, 1997; Zongyu *et al*., 2003; Mazor, 2004; Maduabuchi *et al*., 2006; Demlie *et al*., 2007; Bouchaou *et al*., 2009; Jirakova *et al*., 2009; Kumar *et al*., 2009). In the context of confined reservoirs with groundwaters revealing palaeorecharge and palaeoclimate conditions, several studies have been carried out around the world (Zongyu *et al*., 2003; Edmunds *et al*., 2006; Zhu *et al*., 2007, Jirakova *et al*., 2009; Huneau *et al*., 2011); they pointed out the importance of palaeorecharge and also difficulties in clearly delineating chronology and evolution of recharge history. These isotopes were also used to study the dynamics of overexploited aquifers including the origin of water and the hydraulic connectivity between superposed aquifers (Kamel *et al*., 2005, El-Naqa *et al*., 2007) as well as the origin and process of groundwater contamination in complex systems (Vengosh *et al*., 2002).

In Dakar, the Capital city of Senegal which concentrates about 23% (2,300000 inhabitants of the total population) (estimation DPS, 2004) and large proportion of the industrial activities, water supply is ensured by surface water piped from the Guiers Lake (250 km distant from the capital) and groundwater resources. Among these, the Diass aquifer system contributes to a substantial proportion (36%) of the total water supply distribution due to growing demand as consequence of the rapid demographic growth.

Due to its importance in water supply, several works have been carried out since the early 1970's to better understand the geometry and structure, flow regime and chemical characteristics of this aquifer system (Martin, 1970; Arlab, 1981; 1983; Fall, 1981; Faye, 1983; Faye, 1994). In addition, environmental isotopes are used to infer recharge (BRGM, 1971; IAEA, 1972; OMS, 1972; Faye, 1983; Travi, 1988; Faye, 1994; RAF, 1998; Sarr, 2000). These studies undertaken at the Senegal sedimentary basin scale pointed out the existence of palaeowaters that had been recharged during the late Pleistocene period as well as potential recharge zones in the outcropped Maastrichian aquifer located in the Diass horst and in the South East and East of the basin. In the Diass multilayer system, relatively high tritium contents and high ^{14}C activities in part of the region evidenced modern recharge likely occurring through the upper aquifer and percolation from the Palaeocene aquifer. Water yield of this upper aquifer is limited and it is just exploited by small, dug wells delivering water for some villages. Faye (1994) compiled previous data (BRGM, 1971; IAEA, 1972; OMS, 1972; Faye, 1983; Travi, 1988) and provided additional information by use of long periods radionuclides (series of uranium, ^{4}He, ^{36}Cl) and noble gases (He, Ne, Kr, Xe) to better understand the past and present Maastrichtian system functioning at the Senegal sedimentary basin scale. He argued that the Diass compartment had functioned as a recharge zone for the Maastrichtian aquifer between 4000 and 3000 years BP. This present study particularly focuses to the Diass aquifer to infer its functioning with regards to recharge processes and flow exchange in the context of high exploitation and particular complex geometry setting. In fact, since 1983, abstraction in the five pumping fields to supply Dakar and the localities of Mbour, Sébikotane, Pout increased from 63,000 to 97,000 m³/day for the two aquifers. At present, the total pumping rate is estimated to be 109,000 m^3/d (National Water Society database) in addition to industrial and agricultural activities needs.

This high yield has caused a continuous groundwater level decline (more than 30 m in 50 years) in some parts of the system, a change in the flow regime and quality patterns which are evidenced by salinization of few boreholes located at Sébikotane and Mbour pumping fields (Madioune, 2012).

This high demand and exploitation of the system coincided with the occurrence of drought conditions since the 1970's where inducing deficit in groundwater replenishment as well.

In this system, due to the complexity of the structure and the substantial groundwater abstraction, characteristics such as the hydraulic connectivity between the Palaeocene and Maastrichtian aquifers (vertically and horizontally), the relative significance of present day recharge as well as location of recharge zones need to be investigated.

The present study aims to improve our understanding of groundwater dynamics in order to foster more appropriate groundwater management with regards to high exploitation in the Diass aquifer system scale after 50 years of intensive pumping. Specifically, it intends to: (1) identify the geochemical reactions that take place in the system, (2) infer origin and timing of recharge. This will help to evaluate the recharge mechanism and system functioning needed for management purpose in order to ensure sustainability of the groundwater resources with regards to demand and water quality conservation.

2 Geology and hydrogeology

The study area is located at the western part of Senegal between Dakar and Thiès and extends a surface area of 1340 km² (Figure 1a). It is characterized by a tropical climate with two distinct seasons: a dry season (from November to May) and a rainy season (from June to October). Climate data (precipitation, temperature, relative humidity, insulation and wind speed) during the period from 1977 to 2001 were collected from the Senegal National Meteorological Agency in Dakar Yoff, Thiès and Mbour wheather stations. The average annual precipitation and temperatures are 440 mm and 27°C, respectively.

Rainfall spatial and temporal distribution is highly variable and since the 1970's, a rainfall deficit occurs through most of the Sahel zone (Mahé &Olivry, 1995, Paturel *et* al., 1998, Lebel & Ali, 2009) inducing deficit in groundwater replenishment (Aguillar *et* al., 2010; Madioune, 2012) as well as variations of the hydrologic regime (e.g. Sircoulon, 1987; Hubert *et al.*, 2007, Mahé *et* al.,

2010). Potential and actual evapotranspiration (1977 to 2001) calculated from the Penman method (Allen *et al*., 1998) are 2057 and 371 mm/yr, respectively (Madioune, 2012). The hydrography of the region consists mainly of lakes and fossil valleys (Figure 1a).

The geological structure of the system is updated using hydraulic and petroleum boreholes data (271 in total), previous cross sections (Martin, 1970; Fall, 1981; Faye, 1983) and geological map (1:50,000) established recently by Roger *et al*., (2009). The system is bordered by the Ponty-Kayar fault in the West, the Atlantic Ocean in the North and South and the Thiès fault in the East. Table 1 resumes the geological and hydrogeological characteristics of the system aquifer. The hydrogeological map in Figure 1a presents the top main aquifer.

The Diass aquifer system consists of a complex multilayer structure, compartmentalized by four major faults oriented NE-SW (Figure 1a). These faults configure the region into a horst system with three compartments: the Diass compartment in the center (between Sébikotane and Pout fault) where the Maastrichtian sandstones outcrop surrounded by two Palaeocene karstic limestones compartments (Martin, 1970) namely the Sébikotane compartment in the West (between Ponty-Kayar and Sébikotane fault) and the Pout compartment in the East (between Pout and Thiès fault) (Figure 1a). The geological formations from bottom to top are composed as follow (Martin, 1970; Fall, 1981; Faye, 1983; Roger *et al*., 2009) (Table 1):

- the Maastrichtian formations, they are heterogeneous both laterally and vertically and are composed of clay with interbedded sand, sandstone, calcareous sandstone and clayey sands at the top. Towards the West, they are mainly composed of clayey sediments.
- the Palaeocene consisting of a succession of marly and clayey calcareous and limestone. These latter formation are karstified in the Sébikotane and Pout compartment while in the Western part, they are made of clay and clayey limestone.
- the Eocene formations made up of marl and clay, they cover the Palaeocene limestone in the Sébikotane compartment and in the northern Pout compartment.

- the Mio-Plio-Quaternary sediments composed of clayey sand and laterites, they constitute the top formations (Figure 1b).

Hydraulically, the system is composed of two main aquifers namely the Maastrichtian (lower aquifer) and the Palaeocene (middle aquifer) covered by the superficial quaternary aquifer. Due to the structure of the horst system, these aquifers are also compartmentalized into three hydrogeological units: the Diass compartment in the center, the confined Sébikotane compartment in the West and the confined/unconfined Pout compartment in the East (Figure 1a). Geographically, the Pout compartment is divided into three zones: the Northern Pout zone where the Palaeocene is overlaid by the marly Eocene, the Southern Pout area and the Mbour zone where the Palaeocene layers outcrop.

The Maastrichtian aquifer is composed by an important series of calcareous sandstone, clayey sand and sandstone, separated from the Palaeocene karstified limestone aquifer by the Danian marly limestone. Its thickness increases from West (50 m) to East (450 m). Hydraulic conductivities range from 1.0×10^{-5} to 1.9×10^{-3} m/s and the storage coefficient from 1×10^{-4} to 6×10^{-4} (Table 1) (Géohydraulique & OMS, 1972; Arlab, 1983; Faye,1983; BRGM, 1988; Sarr, 2000). In the Palaeocene karstic limestones aquifer, hydraulic conductivities are highly variable and range from 6.6×10^{-6} to 2.0×10^{-2} m/s. The storage coefficient varies from 1×10^{-4} to 7×10^{-2}. In the Mio-Plio-quaternary aquifer, mean values of hydraulic conductivities and effective porosity are about 1.5×10^{-4} m/s and 20%, respectively (Géohydraulique & OMS, 1972).

3 Data and methods

Piezometric and pumping data series were compiled from databases and technical reports (Senegal Hydraulic Ministry and Water Supply Companies). These data were completed within the present study during the years 2007, 2008. A total of 5 campaigns were carried out for measuring water depth, sampling for chemical (major elements) and isotopic analyses (^{18}O, ^{2}H, ^{3}H, ^{13}C, ^{14}C).

The network comprised 62 piezometers for measuring water depth, 75 boreholes and dug wells for sampling and chemical analysis and 6 climatic stations for rainwater sampling.

The sampling network (Figure 2) was spatially distributed to represent the three aquifers in the three compartments. Rainwater was also collected during the 2008 rainy season (from July to September) for every events at 6 weather stations, Popenguine (76), Mbour (77), Kirène (78), Pout (79), Yenn (81), Thies (80), relatively well distributed in the area. Table 2 resumes the numbers, periods and aquifers sampled. In this paper, we focus the discussions and interpretations on data collected in June 2008 (which is more complete) in addition to isotopic data drawn from previous studies in the region.

Isotopic (^{18}O, ^{2}H, ^{3}H) analyses of the rainwater samples were performed on a biweekly interval basis; rain events smaller than 5 mm were discarded. Prior to groundwater sampling (which was taken in boreholes that were continuously pumped for water supply), on site measurements relative to geographical position, depth to water table, potential Hydrogen (pH), Electrical Conductivity at 25°C (EC), Temperature (T) and alkalinity were conducted at each sampling points. These wells did not need to be purged due to the fact that they are boreholes used for water supply. Physico-chemical parameters (pH, EC, T) were measured using a multiparameter electrochemical analyzer and alkalinity was analyzed on the field. Chemical and isotope analyses of the water samples were performed at the Liege University, Hydrogeology Lab (Belgium) and at the Helmholtz Zentrum München, Institute of Groundwater Ecology (Neuherberg/Germany), respectively.

The major ions (Ca^{2+}, Mg^{2+}, K^{+}, Na^{+}, Cl^{-}, NO_3^{-} and SO_4^{2-}) were measured using flame atomic absorption, potentiometry and titration with charge balance ranging between –4.9 and 2.25% suggesting reliable analyses. Stable isotopes of oxygen and hydrogen were measured using dual-inlet mass spectrometry (Coplen, 1988) with a precision of ± 0.1‰ for $\delta^{18}O$ and ± 1‰ for $\delta^{2}H$. D-excess was calculated as D-excess = $\delta^{2}H - 8\times\delta^{18}O$.

Tritium samples were enriched electrolytically and analysed by the liquid scintillation counting method (Thatcher *et al*., 1977) with 0.7 TU detection limit. Four samples were collected for ^{14}C and

229 ^{13}C analyses which were performed at Gliwice Radiocarbon Laboratory/Institute of Physics/Silesian
230 University of Technology. The analysis of ^{14}C and the ^{13}C are reported in pmc (percent of modern
231 carbon) and in ‰ vs PDB respectively and the analytical errors are ±0.3‰ for ^{13}C and between
232 0.052 and 0.12 pmc for ^{14}C. The carbon analyses were completed with existing data in the region
233 (BRGM, 1971; IAEA, 1972; OMS, 1972; Faye, 1983; Travi, 1988).
234
235 **4 Results and discussions**
236
237 **4.1 Piezometry**
238 Fifteen monitoring wells in the system record variably long term groundwater level since 1965.
239 They feature groundwater depletion in both compartments (Figure 3b, c, d, e). By interpreting this
240 evolution in term of groundwater regime with regards to pumping (Figure 4a, b), piezometric level
241 variations show two types of evolution: seasonal variations (on an annual basis) related to seasonal
242 recharge and long term piezometric level evolution (interannual variations) which reveal two
243 periods of groundwater regime (Figure 4a). A steady state period from 1965 to 1971 with similar
244 seasonal variations indicates recharge (Figure 4a (I)) in both two aquifers. During this period, only
245 the Palaeocene was really exploited (Figure 4b (I)) and its measured head is slightly lower than the
246 Maastrichtian head (Figure 4a (I)).
247 A transient period from 1971 to the present day (Figure 4a (II)) is characterized by a generalized
248 and continuous decline of the groundwater levels due to increasing of exploitation (Figure 4b). With
249 regards to the pumping regime, three stress periods can be distinguished.
250 In stress period (1), which spans from 1971 to 1983, the groundwater regime is characterized by a
251 decline of the levels in the two aquifers. This is likely the result of a decrease in rainfall (37% from
252 1938 to 1983) started in 1970 and increase of the pumping in the Palaeocene while pumping in the
253 Maastrichtian is relatively low and constant (Figure 4b (II, 1)). During this period, the head in the

Maastrichtian is higher and seasonal fluctuations still occurred (Figure 4a (II, 1)) but muted by pumping effects.

The stress period (2), which spans from 1983 to 1992, corresponds to an increase of pumping in the Maastrichtian and a decrease in the Palaeocene (Figure 4b (II, 2)); the hydraulic heads in the two aquifers are relatively in equilibrium (Figure 4a (II, 2)) but are still both decreasing.

In the stress period (3), which spans from 1992 to the present day, pumping from the Maastrichtian is almost constant and maintained at a high level (Figure 4a, b (II, 3)) while it is reduced in the Palaeocene (Figure 4b (II, 3)). The general drawdown of the groundwater level has increased and an inversion of hydraulic head between the two aquifers occurred; here, the Maastrichtian level became lower than the Palaeocene (Figure 4a (II, 3)).

Due to the complex structure of the system into compartments in addition to the low density and location of piezometers in the vicinity of the pumping fields (Figure 5), a reliable piezometric map cannot be drawn. However, hydraulic heads (relative to sea level) measured in June 2008 are highly variable and range between +3.9 m and -47.9 m in the Maastrichtian aquifer (Figure 5b) and between +3.7 m and -36.9 m in the Palaeocene aquifer (Figure 5a) with the lowest values measured at the vicinity of the pumping fields which reveal the dynamic of the system.

4.2 Chemical characteristics

Physico-chemical, chemical and isotopic parameters as well as saturation indexes with respect to calcite and dolomite calculated with PHREEQC (Parkhurst & Appelo, 1999) are statistically resumed in Table 3.

The average temperature increases with depth from 28.7°C to 32.3°C in the upper to the lower aquifers, respectively. The average pH is relatively circumneutral and ranges from 6.6 to 8.3 in the upper aquifer, 6.7 to 7.5 in the Palaeocene aquifer and 6.2 to 7.8 in the Maastrichtian aquifer. Electrical Conductivity (EC) values range between 180-5080 µS/cm, 470-4340 µS/cm and 182-2990 µS/cm for the Quaternary, Palaeocene and Maastrichtian aquifers, respectively. Two groups

280 can be distinguished: (1) Freshwater with conductivities below 1000 µS/cm; this group concerns the
281 majority of samples (83%) representing the wells tapping the upper aquifer except well 3 located
282 upstream the Tanma Lake and wells 12, 13, 14 at Mbour; (2)Saline waters with higher conductivities
283 greater than 1000 µS/cm are located in the Eastern part of the system, in Sébikotane, Mbour and
284 Takhoum areas (wells 24, 25, 28, 37, 40, 53, 56, 61, 73) in both the Palaeocene and Maastrichtian
285 aquifers.
286 Water types defined in the Piper diagram (Figure 6) are Ca-HCO_3 (65%), Ca/Na-Cl (20%), Na-
287 HCO_3 (3%) and Na-Cl (12%). Freshwaters exhibit a dominant Ca-HCO_3 facies, Ca/Na-Cl,
288 Na-HCO_3 while for saline water, Na-Cl and Ca/Na-Cl facies occur.
289 The Ca-HCO_3 facies dominates and represents 65% of the samples. This predominance can be
290 explained by the carbonate matrix of the reservoir where dissolution of calcite (Eq. 1) and dolomite
291 (Eq. 2) combined with the hydrolysis of carbonates (Eq. 3) in the presence of CO_2 are likely the
292 main processes of mineralization.
293

$$CO_2 + H_2O + CaCO_3 \Longleftrightarrow Ca^{2+} + 2HCO_3^- \text{ : calcite dissolution} \quad (1)$$

294 $$CO_2 + H_2O + CaMgCO_3 \Longleftrightarrow Ca^{2+} + Mg^{2+} + 2HCO_3^- \text{ : dolomite dissolution} \quad (2)$$

$$CO_2 + H_2O \Longleftrightarrow H_2CO_3 \Longleftrightarrow HCO_3^- + H^+ \text{: hydrolysis of carbonates} \quad (3)$$

295

296 These processes are confirmed by the alignment of the samples on the calcite-dolomite dissolution
297 line with stoichiometric coefficient of 1:2 (Figure 7a) and by their saturated to supersaturated index
298 values with respect to calcite and dolomite (Figure 7b).
299 In the Palaeocene aquifer, within the Ca-HCO_3 facies, 3 groups can be differentiated (1, 2, 3)
300 characterizing the confined Palaeocene of Sébikotane and Northern Pout and the unconfined
301 Palaeocene of Southern Pout, respectively (Figure 6c). In groups 1 and 2, there is an enrichment of
302 Ca^{2+} and ($\sum HCO_3^- + CO_3^{2-}$) ions and a decrease in Na^+ and Cl^- concentrations towards the main
303 groundwater flow directions as it is shown by the Ca/Na ratio (Figures 6c-1, c-2) and reverse
304 gradient in the Southern Pout compartment (Figure 6c-3).

With regards to the hydrogeological configuration, increasing trend of Ca/Na ratio occurs from the confined to unconfined part of the Palaoecene of Sébikotane and Northern Pout where pumping are highest. The reverse trend of Ca/Na ratio in the unconfined Southern Pout may be related to contribution of calcite dissolution and exchange process from infiltrated water. In the Maastrichtian aquifer, water types evolve laterally from Ca-HCO_3 facies, Na-HCO_3 facies to Na-Cl (Figure 6a). This trend is accompanied by a decrease in Ca^{2+}, ($\sum HCO_3^-$+ CO_3^{2-}) concentrations and an increase of Na^+ and Cl^- in the Diass, Southern Pout, Northern Pout and Mbour directions (Figure 6b). These trends correspond to the passage from freshwater to saline water in some part of the Mbour sectors.

The Palaeocene and Maastrichtian aquifers are characterised by low NO_3^- contents (with respect to drinking water standard) ranging from <0.3 to 28 mg/l with 44% (Palaeocene) and 85% (Maastrichtian) of the wells exhibiting NO_3^- content less than the detection limit (0.3).

The Quaternary upper aquifer is characterized by a Ca/Na-Cl facies, related probably to contribution of rainwater. NO_3^- concentrations reaching 129 mg/l is an indication of the vulnerability of groundwater to pollution and a considerable modern component (Curell *et al.*, 2010) and recharged water from irrigation.

4.3 Isotopes composition of water

Stable isotopes composition of rainwater

The $\delta^{18}O$ values vary from -7.2 ‰ to -2.6 ‰ with an average of -5.3‰ and those of δ^2H from -47‰ to -12‰ with an average of -32‰ (Table 3). Plotted in the conventional $\delta^{18}O$ *vs* δ^2H diagram they define a Local Meteoric Water Line (LMWL) with a regression line $\delta^2H = 7.23 \times \delta^{18}O + 5.9$ (Figure 8a) close to that defined by Travi *et al.* (1987) and the Global Meteoric Water Line (GMWL) (Craig, 1961). This is an indication that rainfalls in Senegal are not evaporated during precipitation due to short and heavy event storms occurring.

The mean monthly weighted $\delta^{18}O$ values of rainwater of all stations correlated with rainfall quantities (Figure 8b) show that low rainfall events in July (beginning of the rainy season) are more enriched than events in August and September which constitutes the maximum of the rainy season.

Stable isotopes composition of groundwater

In order to better understand the system functioning, isotopic data are scrutinized according to superficial (Quaternary), middle (confined/unconfined Palaeocene) and lower (Maastrichtian) aquifers and plotted against the GMWL (Figure 9).

Superficial aquifer

Eighteen samples were analyzed in the Quaternary upper aquifer. $\delta^{18}O$ content range between -5.8 and -4.3‰ and $\delta^{2}H$ between -42 and -31‰, with respective mean values of -5.3‰ and -36‰ (Table 3). These latter values are close to the mean $\delta^{18}O$ and $\delta^{2}H$ values in modern precipitation (-5.3‰ and -32‰). The D-excess (equal to 6.5) compared to that of precipitation (10) suggests a present recharge of rainwater or soil water affected by evaporation or even mixing of irrigation water.

The poorly clustering of the data in the $\delta^{18}O$ *vs* $\delta^{2}H$ diagram that deviated from the GMWL (Craig, 1961) and aligns along an evaporation line of equation: $\delta^{2}H = 4.10\times\delta^{18}O - 14.2$, $R^2 = 0.47$ (Figure 9a) indicates that fractionation by kinetic evaporation and/or mixing of isotopically different rainfall events in addition to agriculture return water flow occurred. In fact agriculture practices are well developed in the region as evidenced by high nitrate contents.

Middle and lower aquifers: Palaeocene and Maastrichtian

For the Palaeocene aquifer, $\delta^{18}O$ content vary from -5.8‰ to -5.0‰ and for $\delta^{2}H$ between -38‰ and -31‰ with an average of -5.5‰ and -35‰, respectively. For the Maastrichtian aquifer, they range from -5.9‰ to -4.3‰ for $\delta^{18}O$ and -38‰ to -26‰ for $\delta^{2}H$, with a mean value of -5.1‰ and -32‰, respectively (Table 3). Plotted in the $\delta^{18}O$ *vs* $\delta^{2}H$ diagram (Figure 9b, 9c), the data of the Palaeocene and Maastrichtian aquifers align on trends parallel and slightly offset the GMWL with respective equations of $\delta^{2}H = 8.03\times\delta^{18}O + 8.89$; $R^2 = 0.63$ and $\delta^{2}H = 7.72\times\delta^{18}O + 7.05$, $R^2 = 0.92$. This June 2008 data used in the paper evidenced distinct scatters of the different aquifers (Figure 9)

with the Palaeocene aquifer exhibiting narrower and slighter range probably evidencing recharge during a cool and humid regime in the past. Scrutinizing the data, it appears that groundwater sampled in the Pout compartment exhibit lightest stable isotopes comparing to those of the Sébikotane compartment which values are wider. On the other side, values of the Maastrichtian aquifer show a large range, aligned on a line parallel and below the GMWL (Figure 9c) but with average D-excess of 8.5.

A clear grouping with regards to geographical zones is not shown, but it appears that a relatively similar lighter isotope composition ($-6<\delta^{18}O<-5‰$) (Figure 9b, 9c) is observed in all Palaeocene (confined and unconfined) and Maastrichtian in Southern Pout and Diass sectors. This similarity may reflect water of same origin and period of recharge. Conversely, a heavier isotope composition ($\delta^{18}O > -5‰$) (Figure 9c) is observed in the Maastrichtian in Mbour and Northern Pout sectors.

This enrichment can be explained by difference in recharge period and/or mixing with recently recharge water by lateral flow along flow paths from the potential recharge zone (located in the Mbour compartment, the northern part of the Pout compartment) towards the piezometric depressions created by pumping or vertical leakage from the more enriched shallow aquifer. The latter is replenished by highly evaporated water ponds created during the rainy season.

The trailing depleted trend along a line parallel and below the GMWL indicates that groundwaters in the Palaeocene and Maastrichtian aquifers are palaeowaters recharged during different periods in the past. This is confirmed by the respective average D-excess values of 8.7 and 8.5 that are 13% and 15% lower than value of modern rainfall (10). As shown by Herczeg *et al*., (2011), in arid and semi-arid zones, groundwater resources are often thought to be largely derived from relatively higher recharge regimes during past wetter climates. Gat (1983), Gat & Issar (1974), Issar *et al*., (1984) reported in Herczeg *et al*. (2011) observed that groundwater stable isotope compositions ($\delta^{18}O$ and $\delta^{2}H$) are more negative than those of weighted mean contemporary rainfall as observed in this paper. Morever, Moser *et al.* (1983) reported by Herczeg *et al*. (2011) evidenced that

381 palaeowaters from arid areas in Saudi Arabia and North Africa are depleted in $\delta^{18}O$ and $\delta^{2}H$ relative
382 to modern rainfall and lie on a palaeowater line that is parallel and below to the global meteoric
383 water line (GMWL). However, Herczeg *et al*. (2011) pointed out some difficulties in interpreting
384 palaeorecharge data which can only be done by comparison of data values and patterns displayed by
385 present day values and ancient period. Despite that, signatures in arid zones are ambiguous due to
386 large variability of rainfall isotopes values, modifications of the isotopic signature at the land
387 surface as well as during infiltration through unsaturated zone which can yield a far greater range of
388 possible final values than those imposed by palaeoclimatic.
389 Ultimately, the heterogeneity of the data shows some variability in patterns and recharge periods.
390 Therefore, it is conceivable to assume that groundwater in the aquifer system is of palaeorecharge
391 origin, and the large range of stable isotopes contents may reflect variable mass flux of isotopically
392 different circulating water (Figure 9c).
393
394 **4.4 Groundwater age and origin**
395 Radioactive isotopes ^{3}H and ^{14}C were used to assess the age of water, recharge periods and probable
396 mixing in the system. The data used for the interpretation are those obtained in this study and from
397 previous studies (IAEA, 1972; Faye, 1983; Travi, 1988; RAF, 1998) (Table 4).
398 Tritium is a valuable tracer for water flow and can give an indication of the relative age of waters
399 varying on a timescale of 50 years before present. It is a naturally occurring isotope of hydrogen not
400 affected by reactions other than radioactive decay. Detectable tritium concentrations in groundwater
401 evidence that recharge has occurred after nuclear bomb test (1952-1953) or mixing had occurred
402 between recent tritiated water and water recharges prior to 1952. ^{14}C can be used as a tracer of the
403 movement and the relative age of water on a timescale ranging from several hundreds to 35,000
404 years. Used in conjunction with ^{3}H, mixing of older groundwater with post nuclear water can be
405 investigated.
406 ***Tritium***

Tritium contents in rainwater measured in June 2008 range from 1.3 to 4.8 TU with a mean value of 2.6 TU (Table 3). They are very close to values measured in the Dakar region in 2008 which range from 1.5 to 2.8 TU with an average of 2.2 TU (Diedhiou, 2011).

In groundwater, tritium contents are mostly below the detection limit (0.7 TU) in percentage of 17%, 87% and 91% for the Quaternary, Palaeocene and Maastrichtian aquifers, respectively. They indicate predominance of old water that has been recharged before 1952 in most of the Palaeocene and Maastrichtian aquifers (Table 3). However, few values above this limit (13% for the Palaeocene and 9% for the Maastrichtian) correspond to mixing between recent and paleowaters (Clark & Fritz, 1997).

In the upper aquifer, the detectable tritium contents -greater than 0.7TU (83%) and ranging from 1.9 to 4.3 TU- are similar to those measured in modern rainwater (Figure 10a) evidencing present recharge. Potential recharge zones of the upper aquifer are identified through the spatial distribution of these high tritium values and are located in the Mbour compartment (cities of Mbour, Ngekokh, Djilakh), in the Diass compartment and in the northern part of the Pout compartment (Mont Rolland, Sao) (Figure 10b). On the other hand, high tritium values greater than 0.7 TU in the Palaeocene (13%) and Maastrichtian (9%) ranged between 1.2 and 1.6 TU and between 1.2 and 1.7 TU, respectively. Occurrence of tritium contents in few wells tapping these aquifers in Northern Pout, Southern Pout and Sébikotane compartments at piezometric depressions (Figure 10b) created by pumping probably reflects a mixing with recent water from upper aquifer through vertical leakage or inferred lateral flow from the potential recharge zones described above.

Carbon isotope (^{13}C and ^{14}C)

The limited carbon data obtained within this study were combined with existing data for age calculation. Our dataset range for ^{13}C between -9.81 and -6.35‰ vs PDB and for ^{14}C between 7.08 and 48.57 pmc (Table 4) and are consistent with data from previous study which are -1.2 to -17.2‰ vs PDB for ^{13}C and between 0.1 to 70.8 pmc for ^{14}C.

Carbon data were recomputed using different age correction models and results show that ages calculated from Fontes & Garnier (1979), Ingerson & Pearson (1964) models are very similar to those computed by IAEA (1972) (Figure 10, Table 4) and a best fit (closer to 1/1 ratio) is obtained between ages calculated from the Fontes & Garnier (1979) model and ages calculated by IAEA (1972). Therefore, the Fontes & Garnier (1979) was used to calculate groundwater age. In fact, this model which is based on the stoichiometric balance of carbonate species, assumes that the carbonate dissolution reactions occur in a closed system where groundwaters, initially in equilibrium with soil CO_2, are isolated from this system before any addition in solution of inactive carbon.

The isotopic content of the Total Dissolved Inorganic Carbon depends not only on the soil CO_2, but also on the isotopic content of the "death" carbon from the aquifer. This model does not take into account an additional contribution of Dissolved Inorganic Carbon other than carbonate dissolution and isotopic exchange. This model is considered in this study due to geochemical reactions that occur in the system characterized by a predominance of carbonate dissolution, and therefore it is a good approximation of the groundwater age of the water.

Our dataset give computed age between actual and 14,500 years BP, while age from previous studies (IAEA, 1972; Faye, 1983; Travi, 1988; RAF, 1998) are from actual to 28,000 years BP (Table 4) and therefore confirm the predominance of palaeowaters in the system. Scrutinizing our dataset they range from 1000 years in Sébikotane and 14,500 years in Northern Pout for two Palaeocene samples and from actual to 730 years for two samples of the Maastrichtian in Mbour and Pout Kirène sectors, respectively.

These results are in accordance with previous studies that give values between 3500 and 17,500 years for the Palaeocene in Sébikotane and 3000-3500 years in the Maastrichtian of Kirène.

The spatial distribution of groundwater age in the Maastrichtian aquifers (Figure 12a) shows sectors of variable ages:

- ✓ groundwater of age greater than 15,000 years BP range between 15,500 and 28,000 years are observed East of the study area and South-West of the system;

- ✓ groundwater of variable age less than 15,000 years BP to actual inequally distributed in the Mbour and Diass sectors.

The few age data obtained in the Palaeocene aquifer show older groundwater age greater than 10,000 years in the Northern part of the Sébikotane and Pout compartment while the relatively recent groundwater from actual to 2600 years BP occurs southward of these compartments.

The analysis of the $\delta^{18}O$ vs radiocarbon age graph (Figure 12b) evidenced two periods of groundwater recharge corresponding to the late Pleistocene period between 10,000 and 20,000 years in the Mbour and Thiès compartment in the eastern part (Figure 12a) and the Holocene period between the present day and 10,000 years in the Diass aquifer system except few samples from Mbour and Northern Pout compartment.

Uncertainties in radiocarbon age dating

Groundwater age estimated in this study with radiocarbon may be associated with uncertainties due to the relative small number of measurements during different periods and the large potential errors associated with model calculation. A major difficulty is estimating the initial ^{14}C concentration at the time of recharge. One of the reasons for this is the variability of chemical and isotopic end members such as soil gas $\delta^{13}C$, $\delta^{14}C$ and pCO2, and assigning carbonate mineral $\delta^{13}C$ and $\delta^{14}C$, which are used in the various ^{14}C correction schemes (Herczeg *et al.*, 2011). Furthermore, the reactions taking place in these systems are quite complex and difficult to accurately assess.

Groundwater age is defined as the average over the water molecules in a sample of the time elapsed since recharge. This simple definition points to a complex reality and a rigorous understanding of groundwater age, then requires a detailed description of how water molecules are transported in a flow regime. A rigorous understanding of groundwater age then requires a detailed description of how water molecules are transported in a flow regime (Bethke & Johnson, 2002). As discuss in Bethke & Johnson (2002) and Park *et al.* (2002) systematic errors induced by the molecular diffusion, dispersion and mixing of different waters arise from application of the radioactive decay equation. When radioactive isotopes are lost from the aquifer by diffusion into confining layers or

484 gained from fine-grained sediments where the rate of subsurface production is high, age calculated
485 from the radioactive decay equation, therefore, is respectively younger and older than the actual
486 age. Sanford (1997) realized a simple model in steady-state flow in regional systems by used of a
487 formula that allows an approximate age correction if necessary for a quick graphical assessment of
488 whether diffusion may be affecting ^{14}C based ages. This study elucidates that a significant loss of
489 ^{14}C occur through molecular diffusion in many types of aquifer system.
490 Furthermore, mixing between aquifer and aquitard by hydrodynamic dispersion may increase or
491 decrease the radioisotopes concentration and lead to respectively younger and older age than the
492 actual age. A mixture of groundwater of differing ages also increases the level of uncertainty
493 associated with groundwater age dating because of the closed system hypotheses used for
494 calculating age. Therefore, applying this method to a mixture of two fluids however, predicts an age
495 that falls systematically younger than the average age of the mixture because the concentration of
496 the radioisotope decays along not a linear but a negative exponential trend. The error becomes
497 especially significant when one fluid is much older than the isotope's half-life.
498 In the context of the Diass aquifer system, due to high pumping, diffusion, dispersion and cross-
499 formational flow are supposed to be high and then allow mixing between younger (superficial
500 aquifer) and older (Palaoecene and Maastrichtian) as well as between deeper aquifers. Therefore,
501 signatures can be enriched or depleted and calculated ages differ from the average age of the mixed
502 waters. Considering the models proposed by Park *et al*. (2002), the groundwater age calculated
503 from the Fontes & Garnier (1979) model which used the radioactive decay equation that did not
504 take in consideration diffusion, hydrodynamic dispersion and mixing of different waters lead to an
505 overestimation of the calculated groundwater ages. The resulting groundwater ages are interpreted
506 in terms of recharge and hydrogeological system functioning and can be therefore taint with
507 uncertainties.
508

509 **4.5 Hydrogeological system functioning**

The radiocarbon and tritium groundwater age indicate that the majority of groundwater pumped in the Palaeocene and Maastrichtian reservoirs in the aquifer system origins from paleowater. However, the high pumping rates in both aquifers which induce vertical to lateral drainance as well as mixing may blur the occurrence of present day rainfall infiltration. At Mbour, the tritium contents (1 to 3.1 TU) and ^{14}C activities (48 pmc) observed respectively in the Quaternary and Maastrichtian aquifers confirm the hypothesis of mixing with recent infiltrated water in this area. On the other hand, in the Northern Pout pumping field, very low activities could be related to the high pumping rate (44,500 m³/day) that induces lateral flow exchanges with the old waters from the eastern part (Figure 12) through the Thies fault according the regional Maastrichtian flow which is from East to West.

5 Conclusions

The Diass horst multilayered aquifer constitutes a complex hydrogeological system and an important reservoir. Increasing exploitation with regards to water demand and the continuous decline of water level are of concern for the water authorities to ensure sustainability of this valuable resource. This study presents results of stable isotope and age dating in an attempt to clarify the origin of recharge water, the age of groundwater resources and flow regime.

Geochemical data mainly indicate low mineralization of the groundwater with EC less than 1000 µS/cm, except for few wells in the Palaeocene at Sébikotane, the Maastrichtian at Mbour and at the Mio-Plio-Quaternary indicating salinisation from saline lakes, marine intrusion. The water type is dominantly Ca–HCO_3 type, reflecting the calcareous and dolomite nature of the aquifers with a predominance of calcite and dolomite dissolution reactions.

Stable isotopes show that the waters had undergone evaporation during infiltration into groundwater in the upper aquifer where present recharge occurs. This aquifer is locally recharged by present precipitation in the Mbour sector (area of Mbour, Ngekokh, Djilakh) and Northern Pout compartment (Mont Rolland and Sao). The results of stable isotopes, age dating using ^{3}H and ^{14}C

536 data confirm that most of the investigated groundwater are palaeowaters and recharge occurred
537 mainly during the Pleistocene and Holocene period between 28,000 years BP to present with a gap
538 between 15,000 and 9000 years BP for the Maastrichtian aquifer. Mixing of old waters and recently
539 recharged (tritiated) waters existent in few exploited boreholes indicating vertical and/or lateral
540 leakage of recent superficial water to deeper aquifers. Calculated groundwater ages may be
541 overestimated because of uncertainties due to mixing of waters of different age. The results of this
542 study, including information about recharge areas and groundwater age, will be used to
543 conceptualize and also to calibrate groundwater flow model, in order to develop and/or refine
544 groundwater management plans for an adequate exploitation of this fragile water resource.
545
546 **Acknowledgements:** This work was supported by the Belgian Technical Cooperation and the
547 "Coopération Française" through the U3E fellowship to Diakher Helene PhD research program at
548 the Liege University. The authors particularly thank staff of the isotopes laboratory at
549 IGOE/Helmholtz Zentrum/Germany and hydrochemistry laboratory at Liege University. Thanks go
550 also to anonymous reviewers for their valuable comments.
551

552 **REFERENCES**

553 Aguiar, L.A.A., Garneau, M., Lézine, A.M., Maugis, P., 2012. Evolution de la nappe des sables
554 quaternaires dans la région des Niayes du Sénégal (1958-1994) : relation avec le climat et les
555 impacts anthropiques. Sécheresse 21: 2, 97-104
556 Allen, R.G., Pereira, L.S., Raes, D., Smith, M., (1998). Crop evapotranspiration – Guidelines for
557 computing crop water requirements. FAO irrigation and drainage paper 56. 300p.
558 Andrews, J.N., Fontes, J.C., Aranyossy, J.F., Dodo, A., Edmunds, W.M., Joseph, A., Travi, Y.,
559 1994. The evolution of alkaline groundwaters in the continental intercalaire aquifer of the Irhazer
560 Plain, Niger. Water Resources Research 30, 45–61.

561 ARLAB, 1981. Alimentation en eau potable de la presqu'île de Dakar. Etude complémentaire du
562 Maastrichtien. Rapport final Projet n°3105070.1542.
563 ARLAB, 1983. Alimentation en eau des I.C.S. Etude complémentaire du Maastrichtien. Rapport
564 technique Arlab 183/83, Arch. DEH.
565 Bethke, C.M., Johnson, T.M., 2002. Groundwater age - Technical commentary. Groundwater 40(4),
566 337-339.
567 Bouchaou, L., Michelot, J.L., Qurtobi, M., Zine, N., Gaye, C.B., Aggarwal, P.K., Marah, H.,
568 Zerouali, A., Taleb, H., Vengosh, A., 2009. Origin and residence time of groundwater in the
569 Tadla basin (Morocco) using multiple isotopic and geochemical tools. Journal of Hydrology 379,
570 323-338.
571 BRGM, 1971. Nappe Profonde du Sénégal (Nappe maastrichtienne). Interprétation des observations
572 périodiques de 1967 à 1970. Interprétation des analyses isotopiques. Fonctionnement hydraulique
573 du système, 71RME 035.
574 Clark, I.D., Fritz, P., 1997. Environmental Isotopes in Hydrogeology. Lewis Publishers, Boca
575 Raton, 311p.
576 Coplen, T.B., 1988. Normalization of oxygen and hydrogen isotope data. Chemical Geology
577 (Isotope Geosciences Section) 72, 293-297.
578 Craig, H., 1961. Isotope variations in meteoric waters. Science 133, 1702–1703.
579 Currell, M.J., Cartwright I., Bradley, D.C., Han, D., 2010. Recharge history and controls on
580 groundwater quality in the Yuncheng Basin, north China. Journal of Hydrology 385, 216-229.
581 Demlie, M., Wohnlich, S., Gizaw, B., Stichler, W., 2007. Groundwater recharge in the Akaki
582 catchment, central Ethiopia: evidence from environmental isotopes ($\delta^{18}O$, $\delta^{2}H$ and ^{3}H) and
583 chloride mass balance. Hydrological Processes 21, 807–818.
584 Diedhiou, M., 2011. Approche multitraceur géochimique et isotopique à l'identification des sources
585 de la pollution nitratée et des processus de nitrification et dénitrification dans la nappe de
586 Thiaroye. Thèse de doctorat unique, Université Cheikh Anta Diop de Dakar, 210p.

587 Direction de la Prévision et de la Statistique/Ministère de l'Economie et des finances, 2004.
588 Projection de population du Sénégal issue du recensement de 2002, 78p.
589 Edmunds, W.M., 2008. Groundwater in Africa-palaeowater, climate change and modern recharge.
590 Applied groundwater studies in Africa, Chapter 18; CRC Press/Balkema, 493p
591 Edmunds, W.M., Ma, J.Z., Aeschbach-Hertig, W., Kipfer, R., Darbyshire, D.P.F., 2006.
592 Groundwater recharge history and hydrogeochemical evolution in the Minqin Basin, North West
593 China. Applied Geochemistry 21, 2148–2170.
594 El-Naqa, A., Al-Momani, M., Kilani, S., Hammouri, N., 2007. Groundwater deterioration of
595 shallow rroundwater aquifers due to overexploitation in Northeast Jordan. Clean Soil Air Water
596 35, 156–166.
597 Fall, M., 1981. Contribution à l'étude hydrogéologique des calcaires paléocènes de Pout et du Lac
598 Tanma. Mem DEA Dpt Géologie Faculté des Sciences et Techniques (FST)/Univ Cheikh Anta
599 Diop. Rapport N°9 Nouvelle série, 43p.
600 Faye, A., 1983. Contribution à l'étude géologique et hydrogéologique du horst de Ndiass et de ses
601 environs (Sénégal occidental). Thèse 3ème cycle Univ. Dakar, 160p + annexes.
602 Faye, A., 1994. Recharge et paléorecharge des aquifères profonds du bassin du Sénégal. Apport des
603 isotopes stables et radioactifs de l'environnement et implication paléohydrologique et
604 paléoclimatique. Docteur es-sciences Thèse de doctorat, 185p.
605 Fontes, J.C., Gasse, F., Andrews, J.N., 1993. Climatic conditions of Holocene groundwater
606 recharge in the Sahel zone of Africa. In: Isotope Techniques in the Study of Past and Current
607 Environmental Changes in the Hydrosphere and the Atmosphere. IAEA-SM-329/59, IAEA,
608 Vienna, Austria, 231–248.
609 Fontes, J.C., Garnier, J.M., 1979. Determination of the initial ^{14}C activity of total dissolved carbon:
610 a review of the existing models and a new approach. Water Resources Research 15(2), 399-413.
611 Géohydraulique & OMS, 1972. Approvisionnement en eau et assainissements de Dakar et ses
612 environs. Etude des eaux souterraines Projet Sénégal 3201 (EX 22), Tome II et III.

613 Gat, J.R., 1983. Precipitation, groundwater and surface waters: control of climate parameters on
614 their isotopic composition and their utilization as palaeoclimatological tools. In: Palaeoclimates
615 and palaeowaters: a collection of environmental isotope studies. Proc. Adv. Gp. Meeting, Vienna,
616 25–28 Nov 1980, pp 3–12, IAEA, Vienna.
617 Gat, J.R., Issar, A., 1974. Desert isotope hydrology: water sources of the Sinai Desert. Geochimica
618 Cosmochimica Acta 38, 1117–1229.
619 Herczeg, A.L., Leaney, F.W., 2011. Review: Environmental tracers in arid-zone hydrology.
620 Hydrogeology Journal 19, 17–29.
621 Hubert, P., Bader, J.C., Bendjoudi, H., 2007. Un siècle de débits annuels du fleuve Sénégal.
622 Hydrological Sciences Journal 52(1), 68-73.
623 Huneau, F., Dakoure, D., Celle-Jeanton, H., Vitvar, T., Ito, M., Traore, S., Compaore, N.F.,
624 Jirakova, H., Le Coustumer, P., 2011. Flow pattern and residence time of groundwater within the
625 south-eastern Taoudeni sedimentary basin (Burkina Faso, Mali). Journal of Hydrology 409, 423–
626 439.
627 Ingerson, E., Pearson, F.J., 1964. Estimation of age and rate of motion of groundwater by the ^{14}C-
628 method. In Recent Researches in the Fields of Hydrosphere, Atmosphere and Nuclear
629 Geochemistry, 263-283, Maruzen, Tokyo.
630 International Atomic Energy Agency, 1972. Report on environmental isotopes studies/
631 Establishment of a Master Plan for water supply and sewerage for Dakar; United States
632 Development Programme (Special fund) project SEN 9, 32p + annexes.
633 Issar, A., Nativ, R., Karnieli, A., Gat, J.R., 1984. Isotopic evidence of the origin of groundwater in
634 arid zones. In: Isotope Hydrology 1983, Proc. Symp. Vienna, IAEA-SM-270/54, IAEA Vienna,
635 pp 85–103.
636 Jirakova, H., Huneau, F., Celle-Jeanton, H., Hrkal, Z., Le Coustumer, P., 2009. Palaeorecharge
637 conditions of the deep aquifers of the Northern Aquitaine region (France). Journal of Hydrology
638 368, 1-16.

639 Kamel, S., Dassi, L., Zouari, K., Abidi, B., 2005. Geochemical and isotopic investigation of the
640 aquifer system in the Djerid-Nefzaoua basin, Southern Tunisia. Environmental Geology 29, 159-
641 170.
642 Kumar, S.U., Sharma, S., Navada, S.V., Deodhar, A.S., 2009. Environmental isotopes investigation
643 on recharge processes and hydrodynamics of the coastal sedimentary aquifers of Tiruvadanai,
644 Tamilnadu State, India. Journal of Hydrology 364, 23-39.
645 Lebel, T., Ali, A., 2009. Recent trends in the Central and Western Sahel rainfall regime (1990–
646 2007). Journal of Hydrology 375, 52-64.
647 Madioune, D.H., 2012. Etude hydrogéologique du système aquifère du horst de Diass en condition
648 d'exploitation intensive (bassin sédimentaire sénégalais) : apport des techniques de télédétection,
649 modélisation, géochimie et isotopie. Thèse de doctorat en sciences de l'Ingénieur/Université de
650 Liège/Faculté des Sciences Appliquées, 325p.
651 Maduabuchi, C., Faye, S., Maloszewski, P., 2006. Isotope evidence of palaeorecharge and
652 palaeoclimate in the deep confined aquifers of the Chad Basin, NE Nigeria. Science of the Total
653 Environment 370, 467-479.
654 Mahé, G., Diello, P., Paturel, J.E., Barbier, B., Karambiri, H., Dezetter, A., Dieulin, C., Rouché, N.,
655 2010. Baisse des pluies et augmentation des écoulements au Sahel : impact climatique et
656 anthropique sur les écoulements du Nakambe au Burkina Faso. Sécheresse 21(1e), 1-6.
657 Mahé, G., Oliviry, J.C., 1995. Variations des écoulements en Afrique de l'Ouest et Centrale de
658 1951 à 1989. Sécheresse 1(6), 109-117.
659 Martin, A., 1970. Les nappes de la presqu'île du Cap-Vert. République du Sénégal. Leur utilisation
660 pour l'alimentation en eau de Dakar. Thèse 3ème cycle Doc. BRGM, 1970. docteur-es-sciences,
661 Dépt de Géologie, Fac. des Scien. et Techn., Univ. C.A.Diop de Dakar, 56p.
662 Mazor, E., 2004. Chemical and Isotopic Groundwater Hydrology. Third ed. Marcel Dekker, New
663 York, 453p.

664 Moser, H., Stichler, W., Trimborn, P., 1983. Stable isotope study on palaeowaters (extended
665 synopsis). In: Palaeoclimates and palaeowaters: a collection of environmental isotope studies.
666 Proc. Adv. Gp. Meeting, Vienna, 25–28 Nov 1980, IAEA, Vienna, pp 201–204.
667 O.M.S., 1972. Etude des eaux souterraines du Sénégal. Rapport Projet SEN 3201, 47p.
668 Paturel, J. E., Servat, E., Delattre, M.O., Lubes-Niel, H., 1998. Analyse de séries pluviométriques
669 de longue durée en Afrique de l'Ouest et Centrale non sahélienne dans un contexte de variabilité
670 climatique. Hydrological Sciences Journal 43 (6), 937-946.
671 Park, J., Bethke, C.M., Torgersen, T., Johnson, T.M., 2002. Transport modeling applied to the
672 interpretation of groundwater ^{36}Cl age. Water Resources Research 38 (5), 1.1–1.15.
673 RAF, 1998. Utilisation des isotopes pour l'étude de la réalimentation des aquifères de la presqu'île
674 du Cap Vert. Rapport Final. Département de Géologie, Université Cheikh Anta Diop, Dakar et
675 SGPRE. Project Modèle A.I.E.A RAF/8/022, 58P + annexes.
676 Sanford, W.E., 1997. Correcting for diffusion in carbon-14 dating of ground water. Groundwater
677 35(2), 357-361.
678 Sarr, B., 2000. Contribution à l'étude hydrogéologique des aquifères de l'Ouest du bassin du
679 Sénégal. Thèse Docteur 3^{éme} cycle. Fac Scien. UCAD, 128p + annexes.
680 Sircoulon, J.H.A., 1987. Variation des débits des cours d'eau et des niveaux des lacs en Afrique de
681 l'Ouest depuis le début du 20ème siècle. The Influence of Climate Change and Climate Variability
682 on the Hydrologic Regime and Water Resources. Proceedings of the Vancouver Symposium,
683 (August 1987), IAHS Publ. no. 168.
684 Thatcher, L., Janzer, V.J., Edwards, R.W., 1977. Methods for determination of radioactive
685 substances in water and fluvial sediments. In: Techniques of Water Resources Investigations of
686 the US Geological Survey. US Government Printing Office, Washington, DC Books 5, Chapter
687 A5, 79-81.

688 Travi, Y., 1988. Hydrogéochimie et hydrogéologie des aquifères fluorés du bassin du Sénégal.
689 Origine et conditions de transport du fluor dans les eaux souterraines. Thèse Sciences. Univ. de
690 Paris Sud (Orsay), 190p.
691 Travi, Y., Gac, J.Y., Fontes, J.C., Fritz, B., 1987. Reconnaissance chimique et isotopique des eaux
692 de pluies du Sénégal. Géodynamique 2, 43-53.
693 Vengosh, A., Gill, J., Davisson, L., Bryant, M., Hudson, G., 2002. A multi-isotope (B, Sr, O, H, and
694 C) and age dating (^{3}H–^{3}He and ^{14}C) study of groundwater from Salinas Valley, California:
695 Hydrochemistry, dynamics, and contamination processes. Water Resources Research 38(1), 9.1-
696 9.17.
697 Zhu, G.F., Li, Z.Z., Su, Y.H., Ma, J.Z., Zhang, Y.Y., 2007. Hydrogeochemical and isotope evidence
698 of groundwater evolution and recharge in Minqin Basin, Northwest China. Journal of Hydrology
699 333, 239–251.
700 Zongyu, C., Jixiang, Q., Jianming, X., Jiaming, X., Hao, Y., Yunju, N., 2003. Paleoclimatic
701 interpretation of the past 30 ka from isotopic studies of the deep confined aquifer of the North
702 China plain. Applied Geochemistry 18, 997-1009.
703

704 **List of figures**

705

706 Figure 1: Hydrogeological map presenting the top main aquifers (a) and cross section of the study
707 area (b) modified from Martin (1970)
708 Figure 2: Map of the study area and location of the groundwater sampling network.
709 Figure 3: Groundwater level monitoring network (a), evolution in time of the measured piezometric
710 level in Sebikotane (b), in Diass (c), in the Southern Pout zone (d), and in the Northern Pout area
711 (e).
712 Figure 4: Evolution of piezometric level with groundwater pumping from 1959 to 2009.
713 Figure 5: Piezometric map of the Palaeocene (a) and Maastrichtian aquifers (b) in June 2008.
714 Figure 6: Piper diagram (a), spatial distribution of Ca/HCO_3 facies type in the Maastrichtian (b) and
715 Palaeocene (c) aquifers, Ca/Na ratio of samples in the Sébikotane (c-1), Northern Pout (c-2) and
716 Southern Pout (c-3) sectors.
717 Figure 7: (Ca^{2+}+Mg^{2+}) vs (HCO^{3}-+$CO3^{2-}$) (a); Calcite and dolomite saturation index (b).
718 Figure 8: $\delta^{2}H$ *vs* $\delta^{18}O$ of precipitation (a), mean monthly weighted $\delta^{18}O$ of all weather stations *vs*
719 monthly rainfall quantities (b).
720 Figure 9: $\delta^{2}H$ *vs*: $\delta^{18}O$ of Quaternary (a), Palaeocene (b) and Maastrichtian (c) aquifers.
721 Figure 10: Tritium vs $\delta^{18}O$ of groundwaters compare with rainwater (a), spatial distribution of
722 tritiated waters (b).
723 Figure 11: Estimation of groundwater radiocarbon age: comparison of IAEA, (1972) corrected age
724 with corrected age calculated from 9 correction models.
725 Figure 12: Spatial distribution of groundwater age (a); $\delta^{18}O$ *vs* radiocarbon age (b) in the
726 Palaeocene and Maastrichtian aquifers.

727

728 **List of tables**

729 Table 1: Geological and hydrogeological characteristics of the aquifer system

730 Table 2: Numbers, periods and aquifers sampled

731 Table 3: Statistic values of physico-chemical, chemical (in mg/l) and isotopic parameters, saturation
732 indexes with respect to calcite and dolomite

733 Table 4: Supplementary data of physico-chemical, chemical (in mg/l) and isotopic parameters,
734 saturation indexes with respect to calcite and dolomite

735

Figure 1

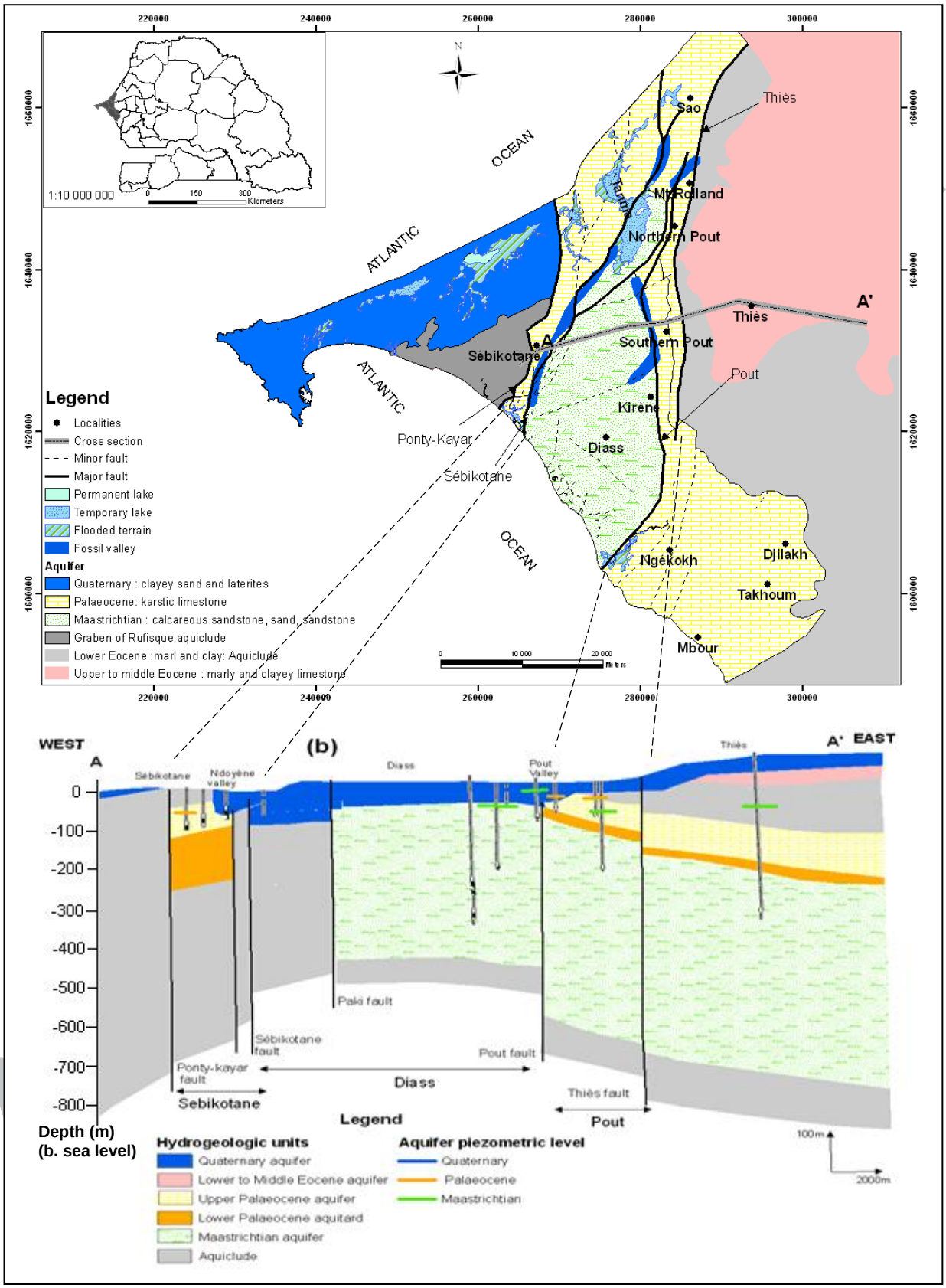

Figure 1: Hydrogeological map presenting the top main aquifer (a) and cross section of the study area (b) modified from Martin (1970)

Figure 2

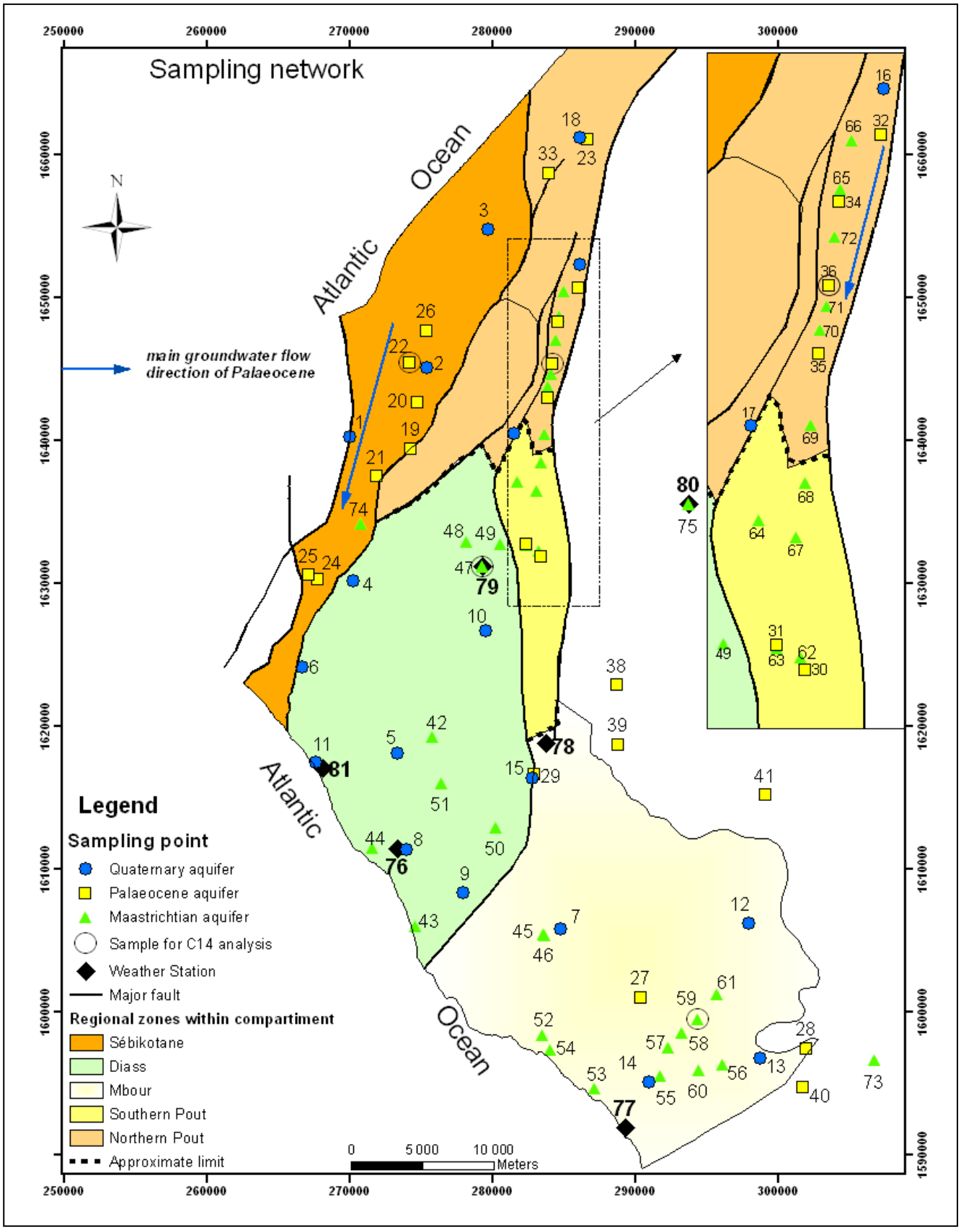

Figure 2: Map of the study area and location of the groundwater sampling network

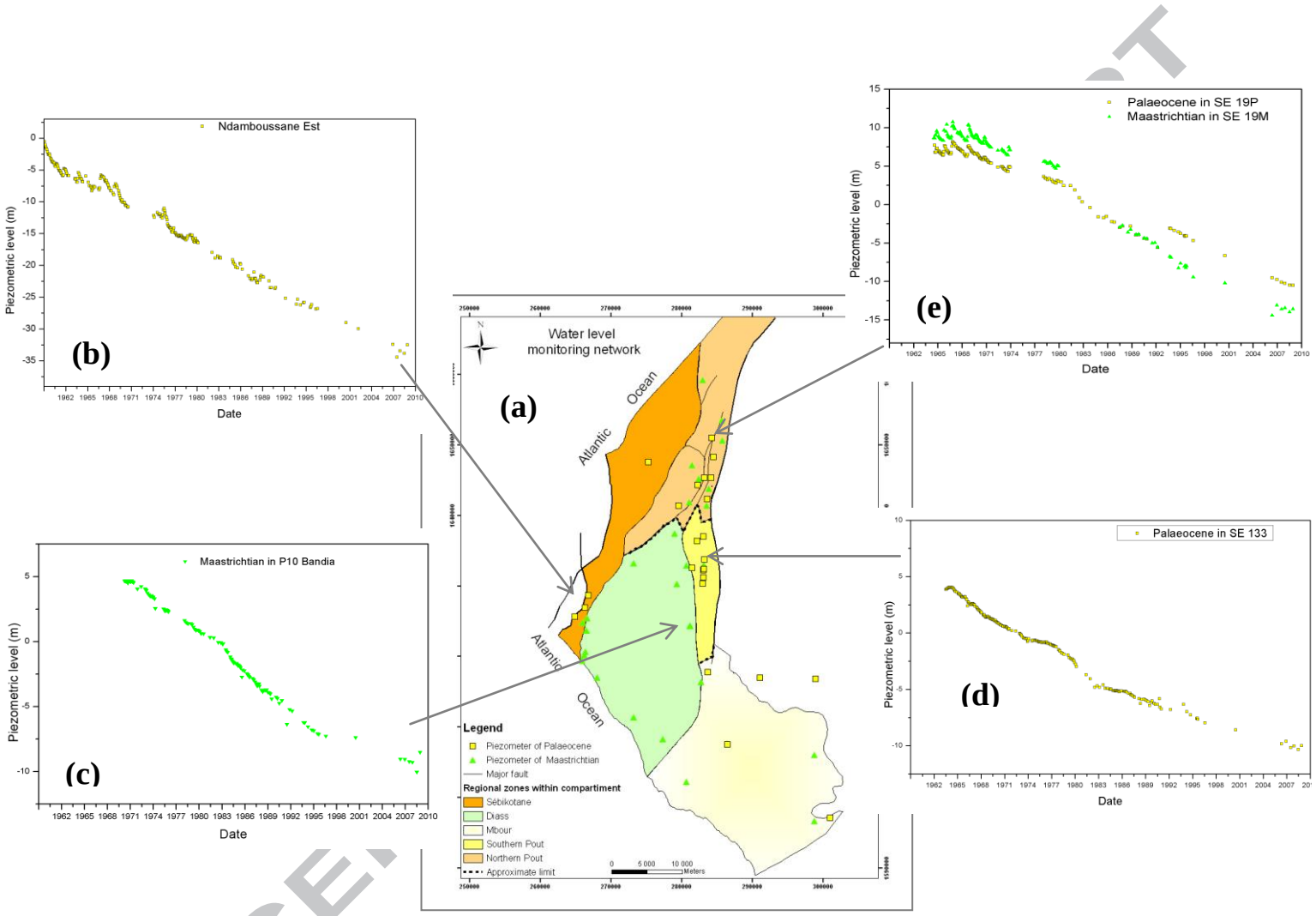

Figure 3: Groundwater level monitoring network (a), evolution in time of the measured piezometric level in Sebikotane (b), in Diass (c), in the Southern Pout zone (d), and in the Northern Pout area (e).

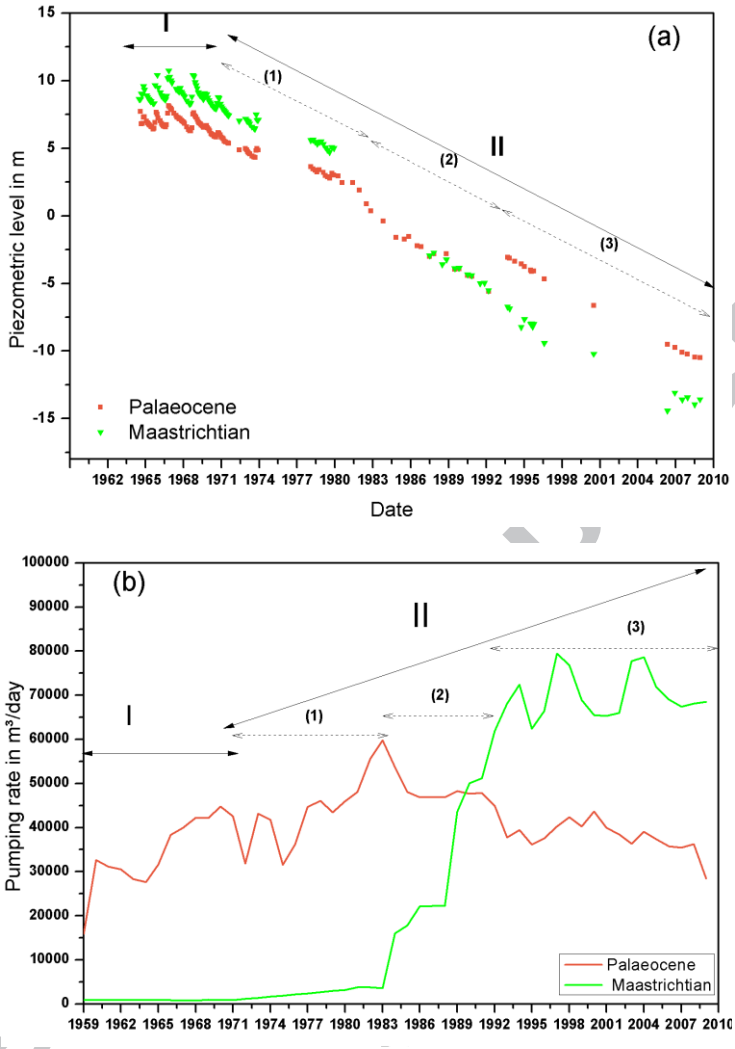

Figure 4: Evolution of piezometric level with groundwater pumping from 1959 to 2009

(a) = Evolution of piezometric level with time; (b) = Evolution of pumping rate with time

I = Steady state period, II = Transient period

(1) (2) (3) are respectively considered as stress periods 1,2 and 3 of the transient period

Figure 5

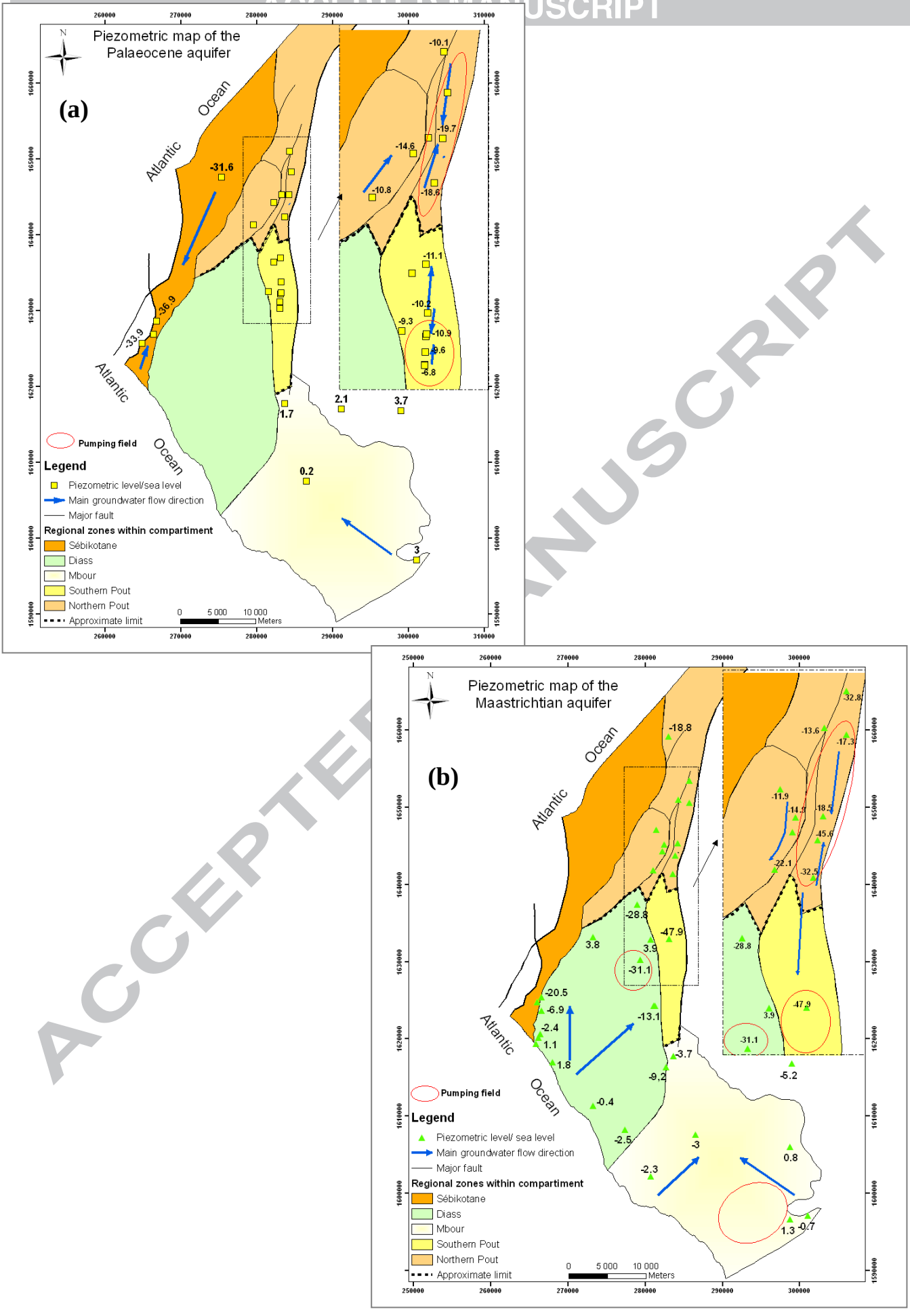

Figure 5: Piezometric map of the Palaeocene (a) and Maastrichtian aquifers (b) in June 2008

Figure 6

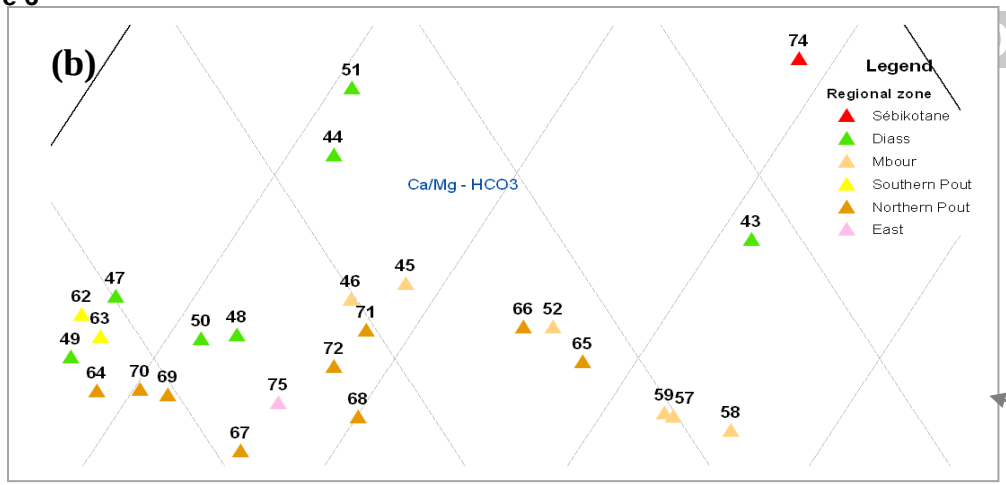

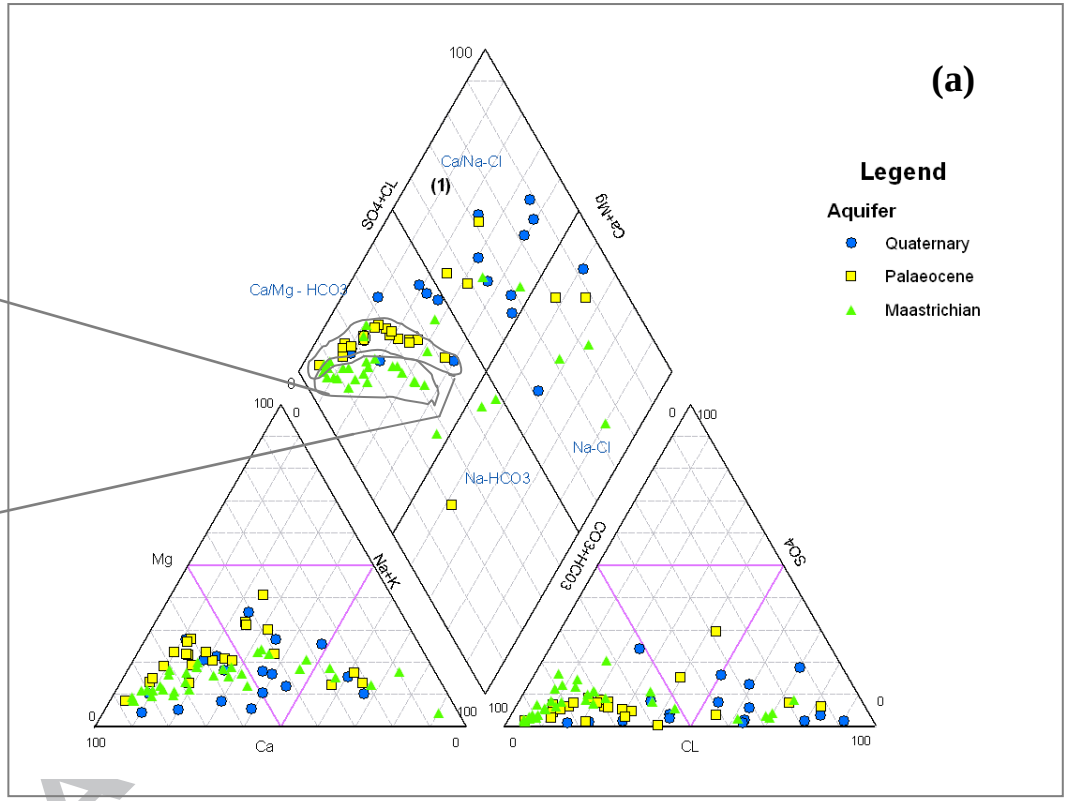

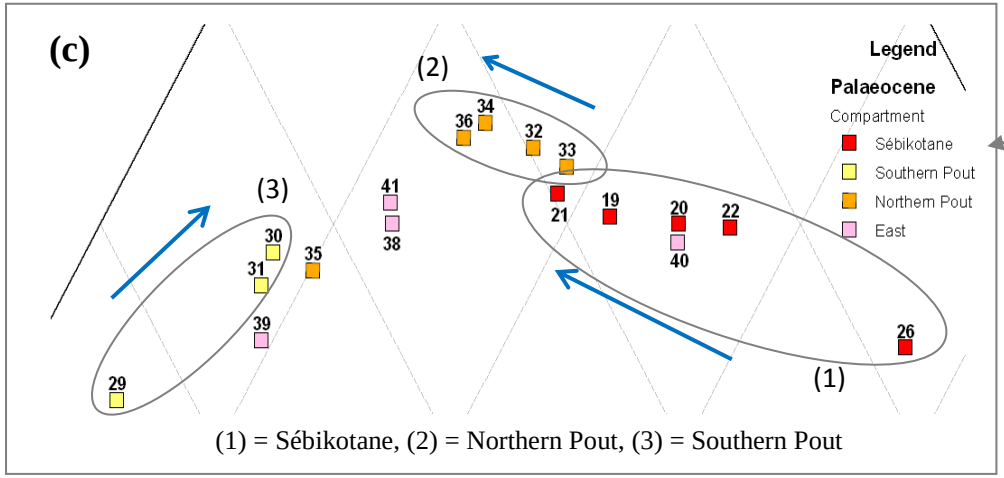

(1) = Sébikotane, (2) = Northern Pout, (3) = Southern Pout

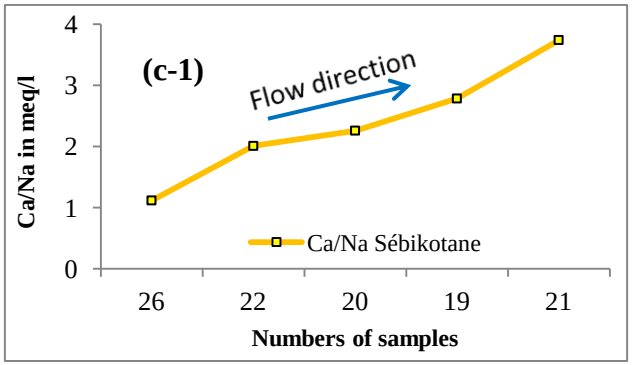

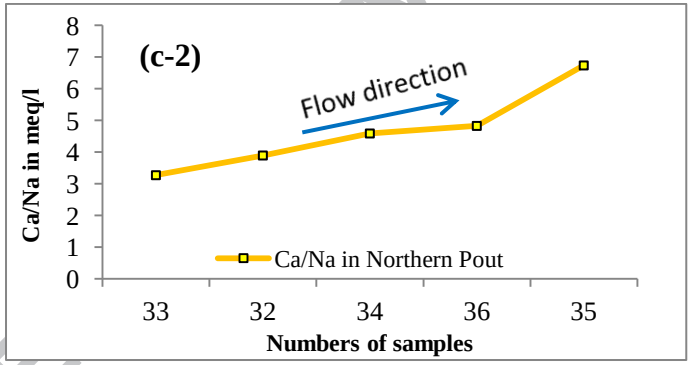

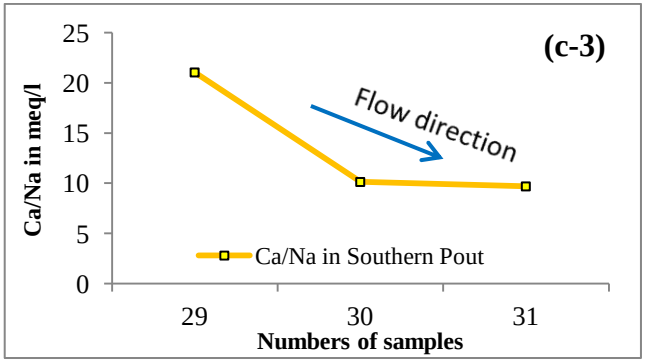

Figure 6: Piper diagram (a), spatial distribution of Ca/HCO_3 facies type in the Maastrichtian (b) and Palaeocene (c) aquifers, Ca/Na ratio of samples in the Sébikotane (c-1), Northern Pout (c-2) and Southern Pout (c-3) sectors

Figure 7

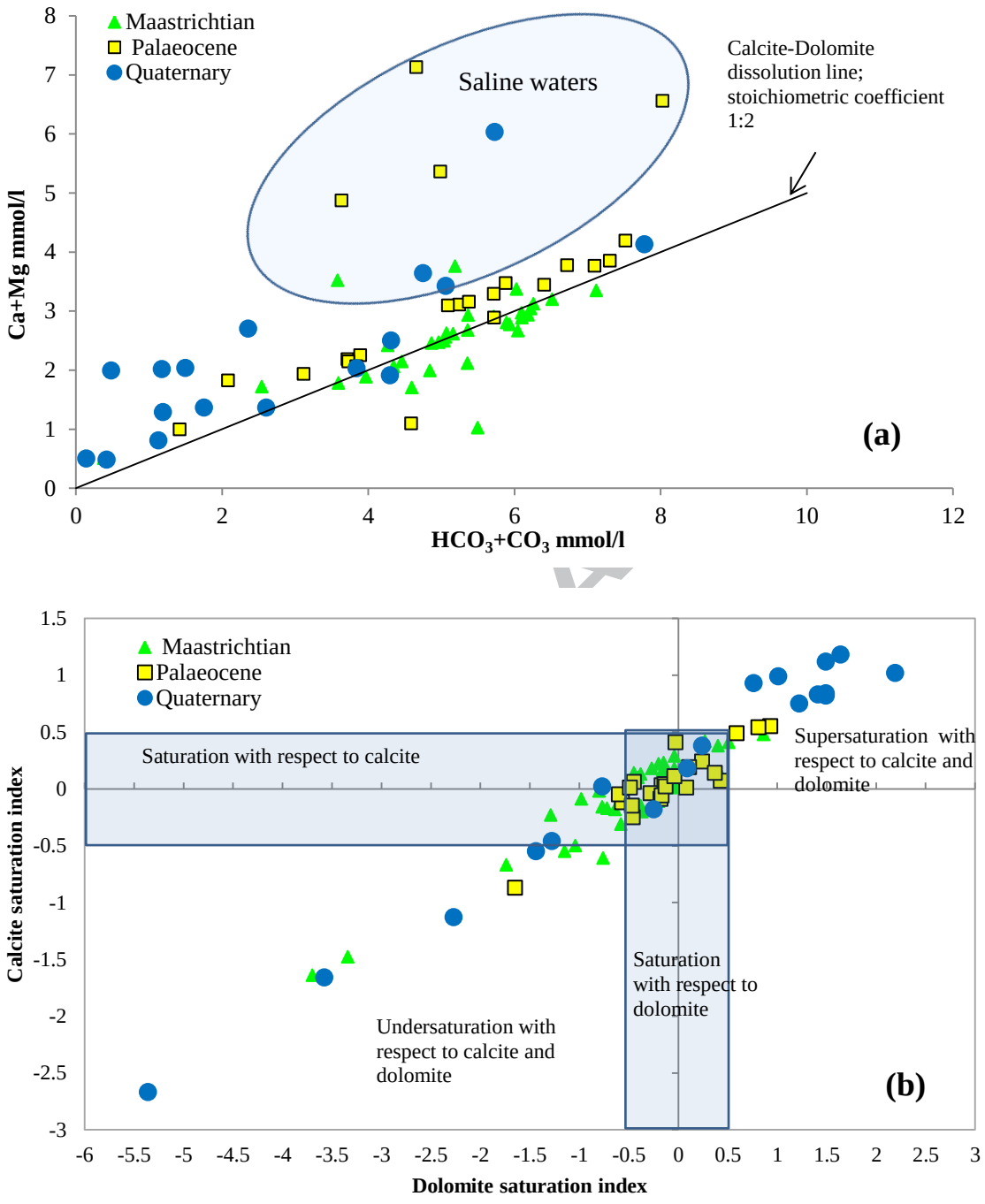

Figure 7: (Ca^{2+}+Mg^{2+}) vs (HCO^{3}-+$CO3^{2-}$) (a); Calcite and dolomite saturation index (b)

Figure 8

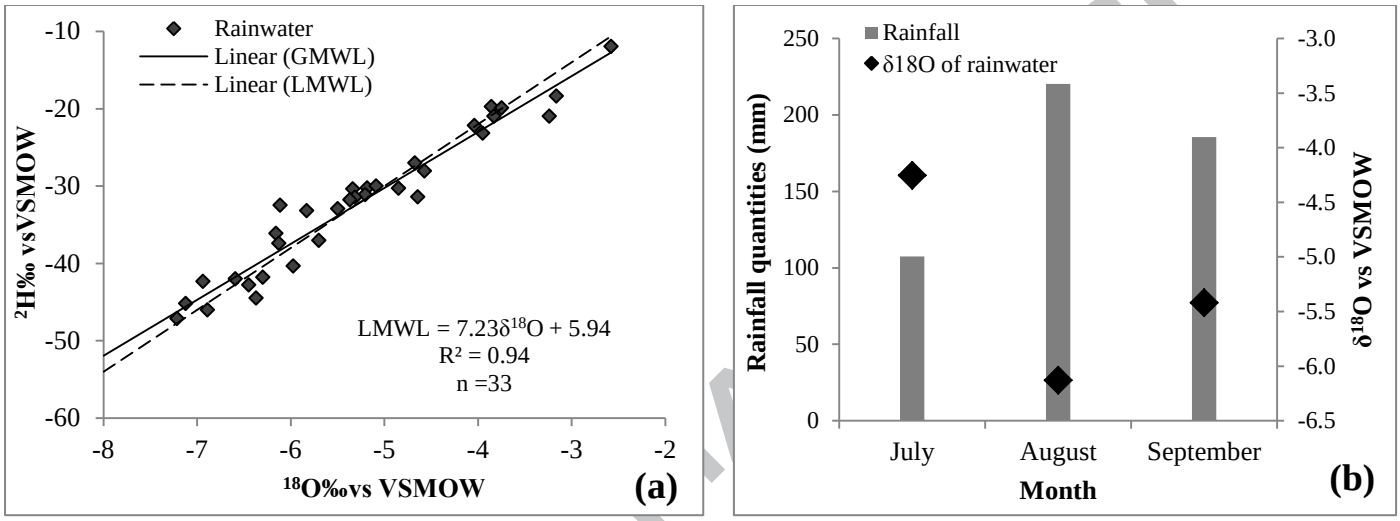

Figure 8: δ^2H *vs* $\delta^{18}O$ of precipitation (a), mean monthly weighted $\delta^{18}O$ of all weather stations *vs* monthly rainfall quantities (b)

Figure 9

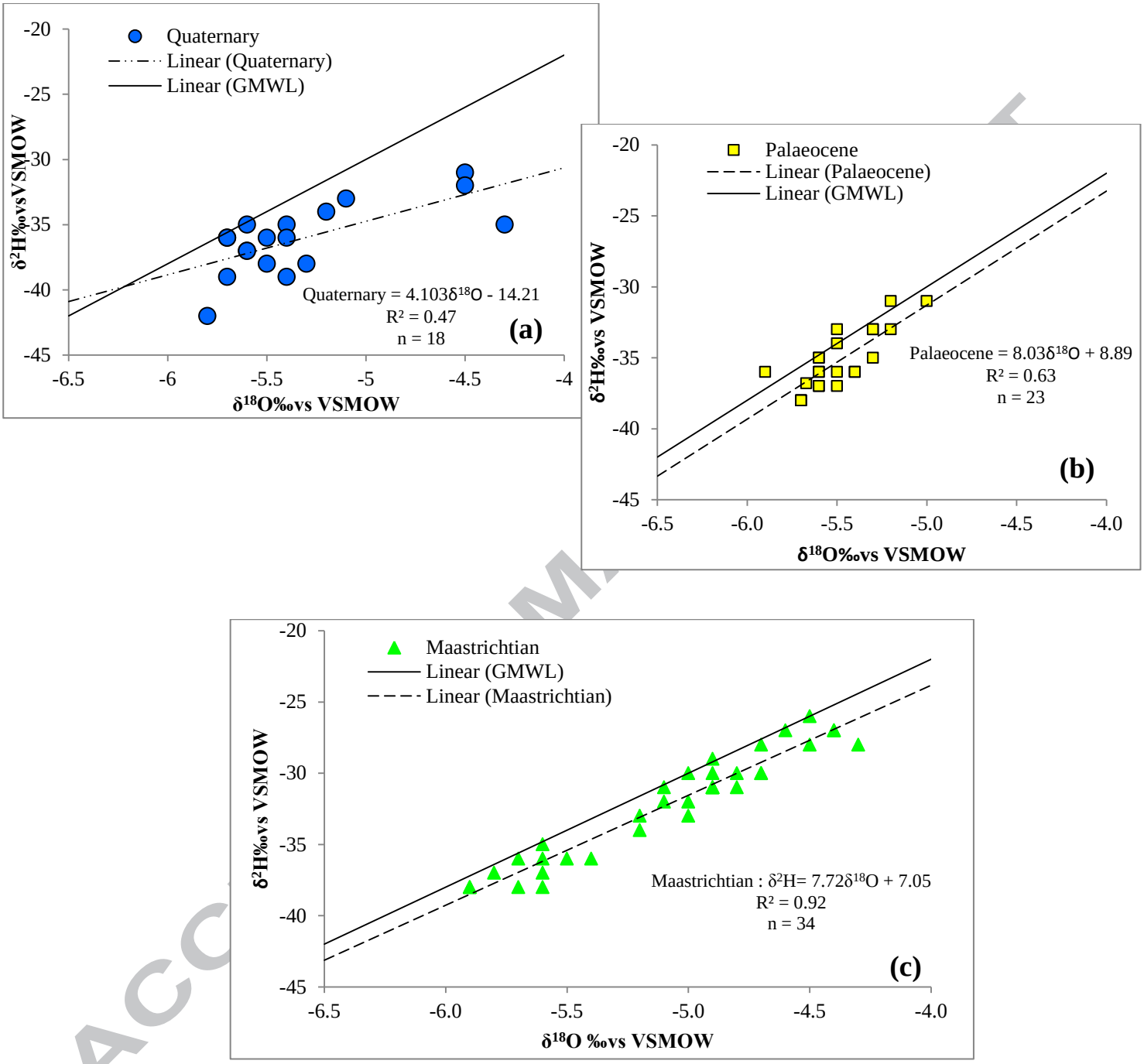

Figure 9: δ^2H *vs* $\delta^{18}O$ of Quaternary (a), Palaeocene (b) and Maastrichtian (c) aquifers

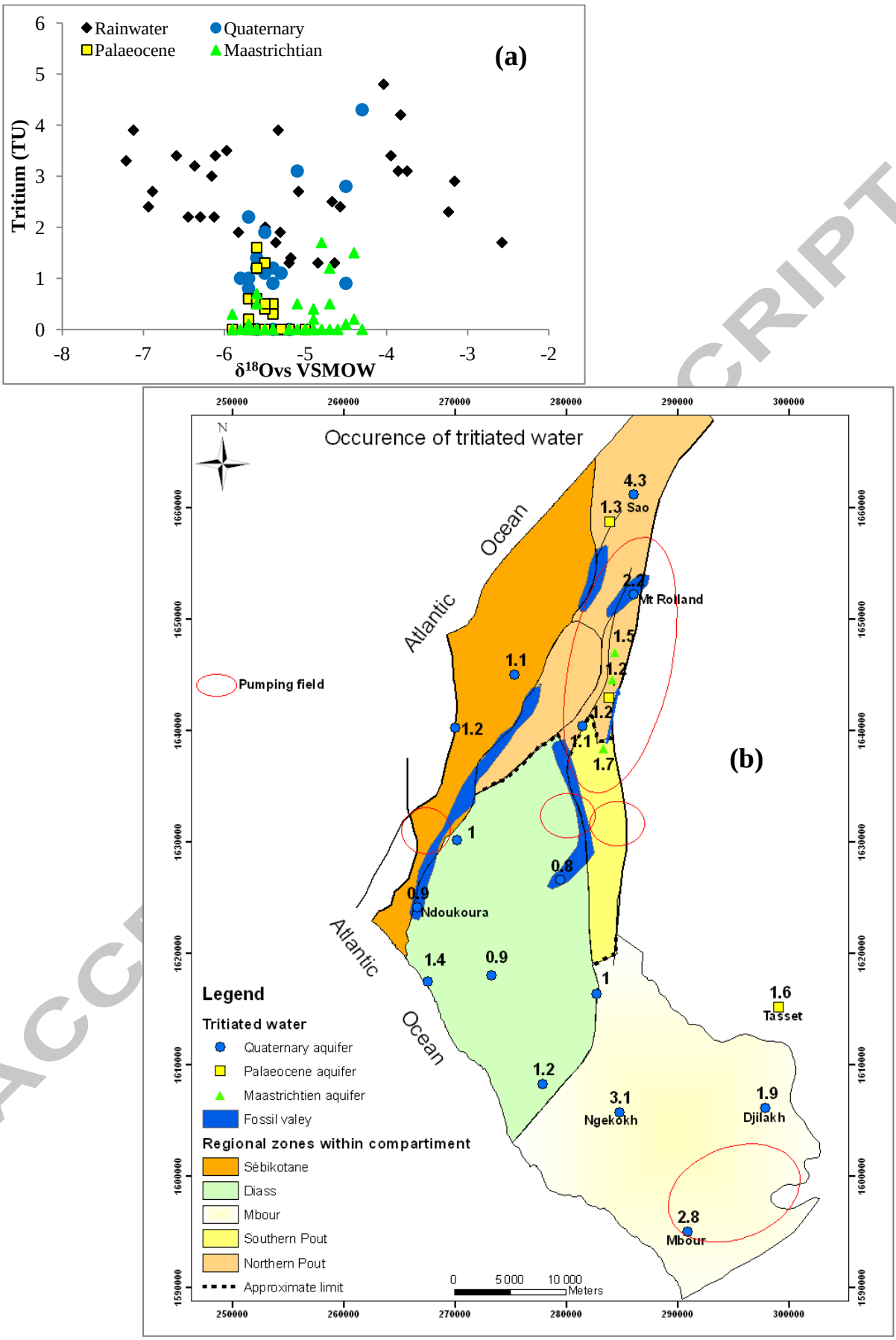

Figure 10: Tritium *vs* $\delta^{18}O$ of groundwaters compared with rainwaters (a), spatial distribution of tritiated waters (b)

Figure 11

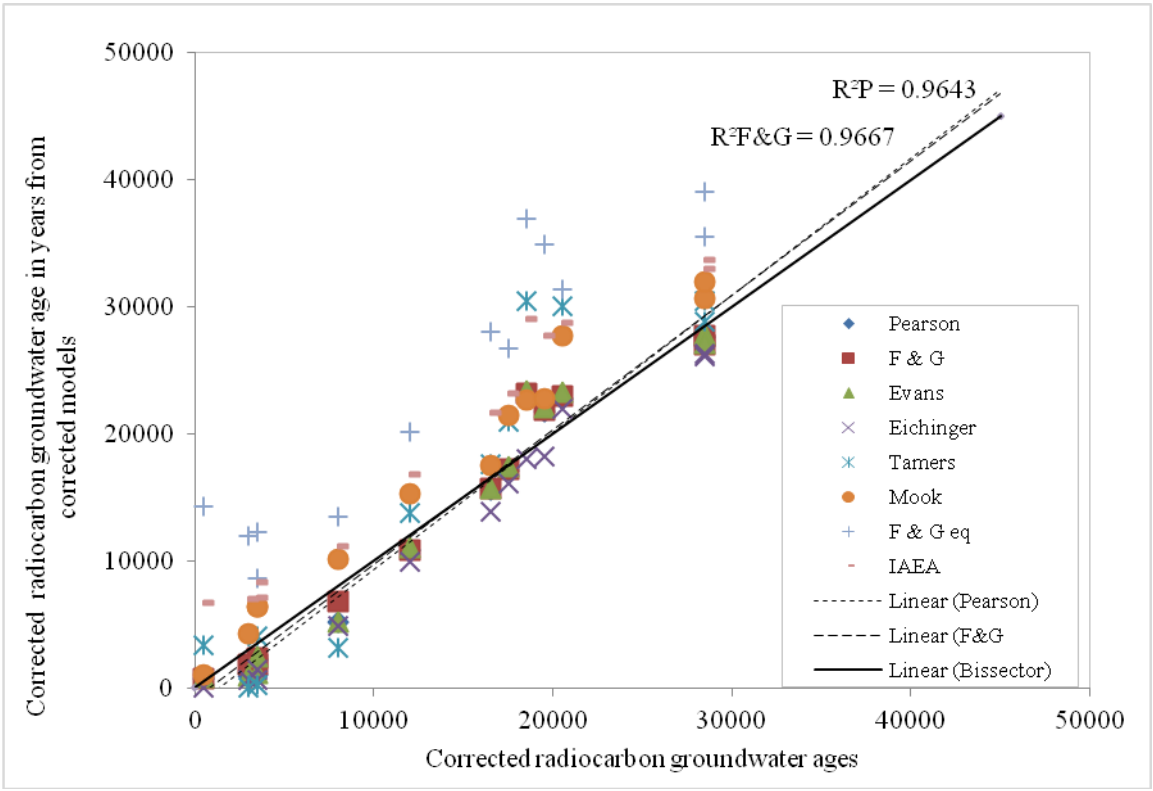

Figure 11: Estimation of groundwater radiocarbon age: comparison of IAEA (1972) corrected age with corrected age calculated from 9 correction models

P = Pearson
Pearson = Ingerson & Pearson (1960)
F & G = Fontes & Garnier (1979)
Evans = Evans *et al* (1979)
Eichinger = Eichinger (1983)
Tamers = Tamers (1975)
Mook = Mook (1980)
F & G eq = Fontes & Garnier (1979) equilibrium
IAEA = IAEA (1972)

Figure 12

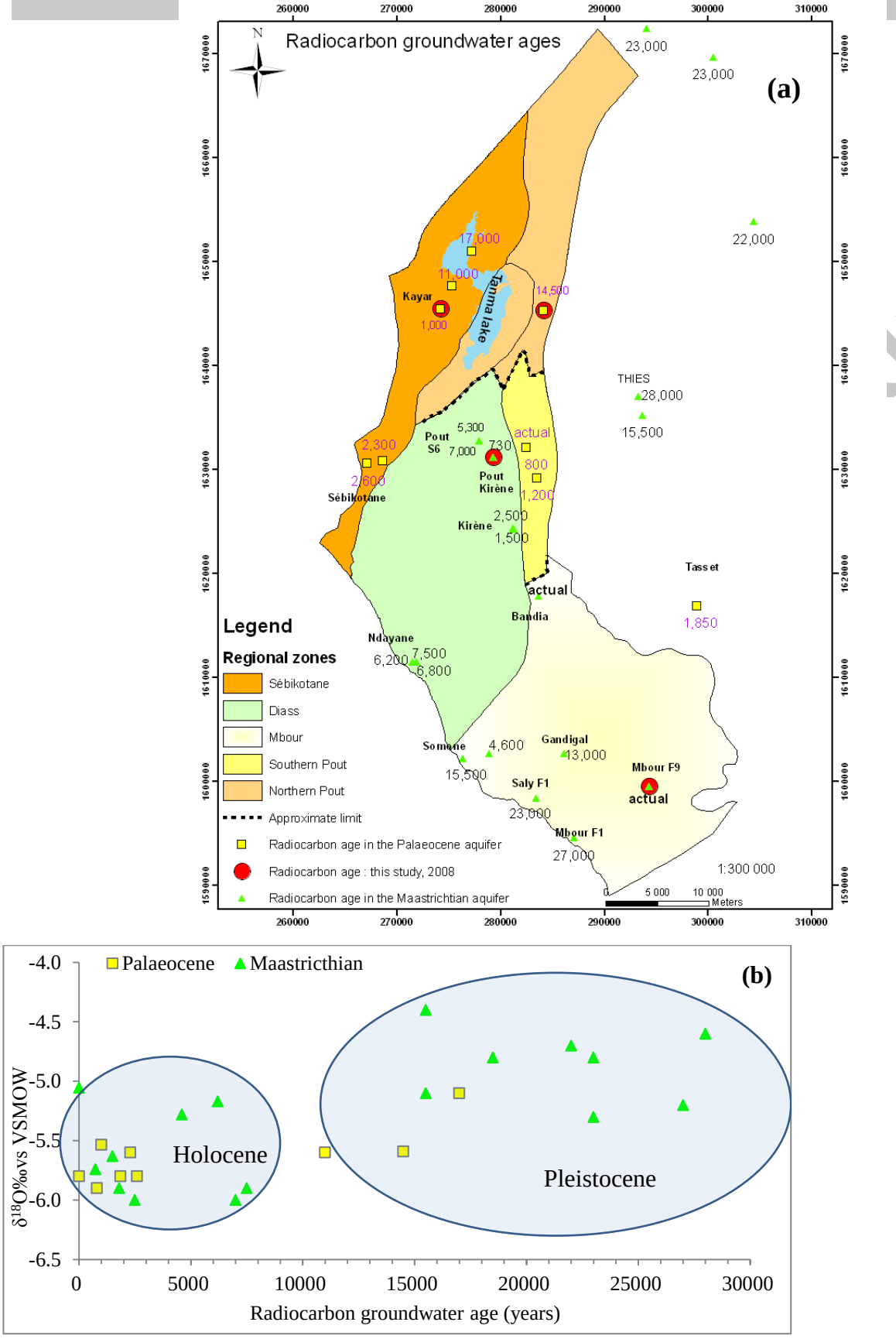

Figure 12: Spatial distribution of groundwater age (a); $\delta^{18}O$ *vs* radiocarbon age (b) in the Palaeocene and Maastrichtian aquifers

Table 1: Geological and hydrogeological characteristics of the aquifer system (K = Hydraulic conductivity; S = Storage coefficient)

Etage		**Dominant lithology / Hydrogeological units /Hydrodynamic properties**					
		Compartments					
		Sebikotane	**Diass**	**Northern Pout**	**Southern Pout**	**Mbour**	**East of the study area**
Mio-Plio-Quaternary		Clayey sand/Aquifer/ $K \approx 1.5\times10^{-4}$ m/s, S = 20%					Clayey sand and laterites/ Aquifer
Eocene	**Upper to Middle**	Marl and clay/Aquiclude	No occurence	Marl and clay/Aquiclude	No occurence		Marly and clayey limestone/Aquifer
	Lower						Marl and clay/ Aquiclude
Palaeocene	**Upper to Middle**	Karstified limestone/Aquifer	No occurence	Karstified limestone /Aquifer/ $K= 6.6\times10^{-6}$ to 2×10^{-2} m/s, $S = 1\times10^{-4}$ to 7×10^{-2}			Not karstified limestone/Aquitard
	Lower (Danian)	Marly and clayey calcareous/ Aquitard		Marly and clayey calcareous / Aquitard			
Maastrichtian	**Upper and Middle**	Clay/Aquiclude	Sandstone, calcareous sandstone and clayey sand /Aquifer $K= 1\times10^{-5}$ to 1.9×10^{-3} m/s, $S = 1\times10^{-4}$ to 6×10^{-4}				
	Lower		Clay with interbedded sand and sandstone/Aquiclude				
Campanian		Clayey sand/Aquiclude					

Table 2: Number of samples, periods and sampled aquifers

Measures	Periods	Number of samples			
		Maastrichtian	Palaeocene	Quaternary	Rainwaters
Piezometric level	April 2007	28	24		
	November 2007	32	24		
	June 2008	35	27	18	
	November 2008	35	26	17	
Chemical	April 2007	34	15		
	November 2007	35	22		
	June 2008	34	23	18	
	November 2008	40	19	17	
	July-August-September 2008				148
Isotopic $\delta^{18}O$, $\delta^{2}H$, ^{3}H ^{14}C, ^{13}C	April 2007	25	14		
	November 2007	35	22		
	June 2008	34	23	18	
	September 2008	2	2	17	
	July-August-September 2008				33

Table 3

Table 3: Statistic values of physico-chemical, chemical (in mg/l) and isotopic parameters, saturation indexes with respect to calcite and dolomite (Q =Quaternary; P =Palaeocene; M=Maastrichtian; W = Well; B = Borehole; R = Rainfall; S = Weather station; min=minimum; max=maximum; b.d.=below detection limit)

Aquifer	Sampling date	Statistic	T(°C)	pH	EC (µS/cm)	Ca^{++}	Mg^{++}	Na^{+}	K^{+}	Cl^{-}	$SO4^{--}$	NO_3^{-}	% NO_3^{-} <0.3	CO_3^{--}	HCO_3^{-}	Free CO_2	SiO_2	Calcite SI	Dolomite SI	TU	2Σ	% TU >0.7	$\delta^{18}O$ (‰)	$\delta^{2}H$ (‰)	$A^{14}C$ (pmc)	$A^{14}C$ error	^{13}C (‰ vs PDB)	Corrected age in years Fontes & Garnier (1979)
R	2008/7-9/	min		5.6	16	1.6	0.1	0.5	0.3	1.1	0.8	0.3		b.d.	1.5	0.3	b.d.			1.3	0.7		-7.2	-47.2				
		max		7.8	362	40.0	2.9	41.9	12.0	40.7	25.3	29.2		0.5	134.6	4.5	4.5			4.8	1.1	100	-2.6	-12.0				
		mean		7.0	92	12.0	0.8	7.3	1.9	8.1	5.8	4.5		0.1	40.2	1.7	0.8			2.6	0.7		-5.3	-32.1				
Q	2008/06	min	26.8	6.6	180	12.2	3.0	10.9	0.1	19.0	0.7	<0.3	5	b.d.	8.5	0.8	1.8	-2.7	-5.4	<0.7	0.7		-5.8	-42.0				
		max	30.2	8.3	5080	431.3	96.2	439.5	12.6	1371.5	108.2	129.7		2.9	473.5	13.2	19.1	1.2	2.2	4.3	0.8	83	-4.3	-31.0				
		mean	28.7	7.7	947	89.1	17.5	71.5	4.0	176.2	23.9	35.7		0.9	184.5	2.5	9.2	0.1	-0.1		0.7		-5.3	-36.0				
P	2008/06	min	28.8	6.7	474	24.8	5.9	5.8	0.7	10.4	1.6	<0.3	44	0.7	126.6	0.9	13.6	-0.9	-1.7	<0.7	0.7		-5.9	-38.0	7.1	0.05	-9.4	1,000
		max	34.2	7.5	4340	174.9	70.2	620.4	10.0	1194.0	182.9	21.0		5.2	487.2	3.5	75.1	0.6	0.9	1.6	1.5	13	-5.0	-31.0	38.7	0.11	-8.8	14,500
		mean	30.9	7.1	999	93.7	25.2	74.3	2.8	148.7	34.8	4.3		1.9	311.3	2.1	30.4	0.1	-0.1		0.9		-5.5	-35.0	22.9	0.08	-9.1	7,750
M	2008/06	min	27.6	6.2	182	16.3	2.4	6.4	1.1	10.4	1.3	<0.3	85	b.d.	23.2	0.8	12.1	-1.6	-3.7	<0.7	0.6		-5.9	-38.0	41.8	0.11	-9.8	actual
		max	38.2	7.8	2990	117.4	58.5	472.3	21.5	764.6	118.2	28.2		3.4	432.6	3.8	54.0	0.5	0.9	1.7	1.5	9	-4.3	-26.0	48.6	0.12	-6.4	730
		mean	32.3	7.0	818	76.7	13.9	64.5	6.1	87.8	28.4	1.8		1.8	301.4	2.2	24.7	-0.1	-0.5		1.0		-5.1	-32.0	45.2	0.12	-8.1	
M	1969-1995	min	29.0	5.8											79.3					0.1			-6.0	-36.0	0.1	0.3	-17.2	1,500
		max	33.4	8.9											488.0					19.3			-4.4	-20.3	70.8	1.3	-1.2	28,000
		mean	31.5	7.0											268.4					5.7			-5.2	-29.7	24.0	0.7	-11.4	12,585
P	1969-1995	min	29.9	6.5											192.2					0.3			-6.4	-39.0	4.5		-12.6	800
		max	32.4	7.6											416.0					15.4			-5.1	-34.0	56.2		-7.5	17,000
		mean	31.2	7.1											299.7					3.2			-5.8	-36.3	37.3		-10.6	5,250

Table 4

Table 4 : Physico-chemical, chemical (in mg/l) and isotopic parameters, saturation indexes with respect to calcite and dolomite (Q =Quaternary; P =Paleocene; M=Maastrichtian; W = Well; B = Borehole; R = Rainfall; S = Weather station ; N.Pout =Northern Pout ; Southern Pout; East = East of the study area)

ot

Num	Samples	Aquifer	Sampling points	Compartment	Sampling date	Sampling depth	T(°C)	pH	EC (µS/cm)	Ca^{++}	Mg^{++}	Na^{+}	K^{+}	Cl^{-}	$SO4^{--}$	NO_3^{-}	CO_3^{--}	HCO_3^{-}	Free CO2	SiO_2	Calcite SI	Dolomite SI	Facies type	TU	2Σ	$\delta^{18}O$ (‰)	$\delta^{2}H$ (‰)	$A^{14}C$ (pmC)	$A^{14}C$ error	$\delta^{13}C$ (‰ vs PDB)	Corrected age in years Source	IAEA, 1972	Fontes & Garnier
1	Bayakh	Q	W	Sebi	2008/06	-	28.5	7.6	602	43.9	22.8	28.1	2.6	114.5	33.8	1.5	0.2	91.0	1.5	15.9	-0.18	-0.25	Ca/Na-Cl	1.2		-5.4	-39				This study		
2	Diender	Q	W	Sebi	2008/06	-	27.6	7.9	486	45.4	5.7	34.7	12.6	58.2	17.4	2.6	0.8	158.1	1.3	10.5	0.38	0.24	Ca/Mg-HCO3	1.1		-5.3	-38				This study		
3	Gadiaga	Q	W	Sebi	2008/06	-	27.4	8.3	1442	73.9	43.6	155.6	3.9	254.9	108.2	<0.3	2.9	286.5	1.1	16.3	1.02	2.19	Ca/Na-Cl	< 0.7		-5.2	-34				This study		
4	Tène Thomas	Q	W	Diass	2008/06	-	29.8	7.6	253	24.9	4.6	10.9	4.2	19.0	25.6	1.0	0.1	69.2	1.3	6.0	-0.55	-1.44	Ca/Mg-HCO3	1.0		-5.7	-36				This study		
5	Mbayar	Q	W	Diass	2008/06	-	28.4	8.2	488	75.9	3.2	21.1	4.3	40.1	3.1	1.3	1.9	232.5	1.1	5.2	0.99	1.01	Ca/Mg-HCO3	0.9		-4.5	-31				This study		
6	Ndoukoura	Q	W	Diass	2008/06	-	27.7	7.9	374	39.8	9.2	17.5	1.1	49.8	6.1	17.9	0.5	106.2	0.9	7.2	0.18	0.09	Ca/Mg-HCO3	0.9	0.7	-5.4	-35				This study		
7	Ngekokh	Q	W	Mbour	2008/06	-	28.7	7.7	777	73.3	4.5	60.1	1.0	181.9	5.2	17.4	0.2	71.5	1.0	9.0	0.02	-0.77	Ca/Na-Cl	3.1	0.7	-5.1	-33				This study		
8	Popenguine	Q	W	Diass	2008/06	-	26.8	8.0	764	122.1	9.2	14.0	5.3	83.3	6.4	9.3	1.9	307.1	2.0	8.7	1.12	1.49	Ca/Mg-HCO3	< 0.7		-5.6	-35				This study		
9	Sorokhassap	Q	W	Diass	2008/06	-	28.7	6.6	314	12.2	4.7	34.8	0.6	57.2	1.4	46.0	0.0	8.5	1.4	5.9	-2.67	-5.36	Na-Cl	1.2		-5.6	-37				This study		
10	Thiambo	Q	W	Diass	2008/06	-	29.1	8.0	548	95.2	3.0	12.9	1.6	30.9	3.0	25.5	1.3	261.8	2.0	9.7	0.93	0.76	Ca/Mg-HCO3	0.8		-5.7	-36				This study		
11	Yenn	Q	W	Diass	2008/06	-	29.6	7.4	494	39.9	7.1	47.8	2.5	86.0	10.7	47.4	0.1	72.9	1.9	4.2	-0.46	-1.28	Ca/Na-Cl	1.4		-5.6	-37				This study		
12	Djilakh	Q	W	Mbour	2008/06	-	29.9	7.8	1821	214.9	16.4	117.0	8.0	380.0	16.2	39.9	1.3	348.4	3.5	8.9	1.18	1.64	Ca/Na-Cl	1.9	0.7	-5.5	-38				This study		
13	Louly. B	Q	W	Mbour	2008/06	-	29.3	7.3	5080	431.3	96.2	439.5	11.6	1371.5	77.3	129.7	0.4	375.9	13.2	19.1	0.83	1.41	Ca/Na-Cl	< 0.7		-5.4	-36				This study		
14	Mbour	Q	W	Mbour	2008/06	-	29.7	8.2	1231	52.8	14.4	179.0	6.6	213.9	40.6	35.7	2.1	260.2	1.2	1.8	0.82	1.49	Na-Cl	2.8	0.7	-4.5	-32				This study		
15	Bandia.S	Q	W	S. Pout	2008/06	-	29.1	7.1	180	14.1	3.1	12.0	1.5	26.6	0.7	22.7	0.0	25.5	1.5	7.7	-1.66	-3.58	Ca/Na-Cl	1.0		-5.8	-42				This study		
16	Darou.Al	Q	W	N. Pout	2008/06	-	29.3	7.6	838	115.8	30.2	24.2	0.1	32.0	31.7	7.8	1.0	473.5	8.7	7.5	0.84	1.49	Ca/Mg-HCO3	2.2	0.8	-5.7	-39				This study		
17	Ngomène	Q	W	N. Pout	2008/06	-	30.2	8.1	656	80.8	16.6	28.9	0.9	67.2	5.7	124.9	1.0	143.0	0.8	10.8	0.75	1.22	Ca/Mg-HCO3	1.1		-5.5	-36				This study		
18	Sao	Q	W	N. Pout	2008/06	-	27.2	7.2	703	46.8	19.9	48.4	3.1	105.2	36.6	111.2	0.0	29.2	1.4	10.7	-1.13	-2.27	Ca/Na-Cl	4.3	0.7	-4.3	-35				This study		
19	Bayakh	P	B	Sebi	2008/06	-	31.3	7.5	551	64.4	13.9	26.6	2.2	47.7	20.9	2.0	1.6	227.2	1.3	18.2	0.24	0.24	Ca/Mg-HCO3	< 0.3	1.0	-5.2	-31				This study		
20	Diender	P	B	Sebi	2008/06	202-242	30.6	7.2	596	65.2	15.2	33.2	1.9	62.4	15.9	<0.3	1.2	236.4	1.7	18.5	0.03	-0.17	Ca/Mg-HCO3	<0.5	1.0	-5.3	-33				This study		
21	F1 K. Sega	P	B	Sebi	2008/06	160-189	31.3	7.1	542	73.2	8.8	22.5	1.8	45.5	16.7	2.4	2.1	224.8	0.9	29.1	-0.05	-0.60	Ca/Mg-HCO3	0.1	0.9	-5.6	-35				This study		
22	Kayar	P	B	Sebi	2008/06	180-210	31.7	7.2	595	62.0	14.6	35.5	2.3	67.2	14.1	<0.3	0.9	226.1	2.2	19.1	-0.04	-0.28	Ca/Mg-HCO3	<0.3	1.0	-5.3	-35	38.7	0.1	-9.4	This study		1,000
23	Sao	P	B	N. Pout	2008/06	100-130	28.8	7.4	536	41.9	19.0	25.8	3.0	66.0	34.5	<0.3	0.7	126.6	0.9	20.3	-0.25	-0.46	Ca/Na-Cl	0.0	0.8	-5.2	-33				This study		
24	Sebi F2	P	B	Sebi	2008/06	49-72	30.8	6.7	2640	149.8	39.5	332.1	6.9	660.5	93.5	<0.3	1.6	302.7	2.2	16.4	-0.15	-0.47	Na-Cl	<0.3	0.8	-5.6	-35				This study		
25	Sebi F3	P	B	Sebi	2008/06	65-82	31.2	6.8	4340	174.9	67.2	620.4	7.5	1194.0	127.5	<0.3	1.0	283.3	3.2	61.2	-0.09	-0.18	Na-Cl	<0.2	0.7	-5.5	-33				This study		
26	Thieudeum	P	B	Sebi	2008/06	93-180	31.8	7.2	670	53.4	17.9	55.0	3.1	96.8	1.6	0.7	1.4	232.5	1.5	15.7	-0.06	-0.17	Ca/Mg-HCO3	<0.4	0.9	-5.3	-33				This study		
27	K. Meissa	P	B	Mbour	2008/06	206-230	32.1	6.7	557	24.8	11.5	76.8	8.2	29.9	17.4	0.5	2.1	277.4	1.4	13.6	-0.87	-1.65	Na-HCO3	0.2	0.8	-5.7	-37				This study		
28	Louly Ng	P	B	Mbour	2008/06	18-53	30.8	6.8	1914	147.3	70.2	139.1	2.3	386.8	36.0	2.3	2.6	487.2	3.5	69.9	0.10	0.37	Ca/Na-Cl	0.3	0.7	-5.4	-36				This study		
29	Bandia	P	B	S. Pout	2008/06	58-80	30.9	7.2	556	106.1	5.9	5.8	1.2	10.4	6.0	<0.3	1.8	347.4	2.6	19.8	0.41	-0.03	Ca/Mg-HCO3	<0.4	0.8	-5.9	-36				This study		
30	PS3	P	B	S. Pout	2008/06	-	29.6	6.8	753	128.6	13.8	14.6	1.1	28.4	26.9	6.1	1.9	408.3	3.4	18.2	0.06	-0.45	Ca/Mg-HCO3	0.6	0.8	-5.7	-38				This study		
31	PS5	P	B	S. Pout	2008/06	-	30.3	6.8	699	115.4	13.7	13.7	1.1	29.5	17.0	9.8	2.7	388.3	2.2	25.1	0.01	-0.49	Ca/Mg-HCO3	0.6	0.8	-5.7	-38				This study		
32	Mt Rolland	P	B	N. Pout	2008/06	61-79	30.4	6.8	723	96.2	17.3	28.4	1.3	59.0	30.2	6.2	1.6	318.5	2.4	27.3	-0.12	-0.57	Ca/Mg-HCO3	0.5	0.8	-5.6	-37				This study		
33	Noto G.Diama	P	B	N. Pout	2008/06	75-109	30.4	7.4	474	55.5	13.3	19.5	1.8	41.0	13.1	7.7	1.0	189.4	1.4	21.5	0.04	-0.14	Ca/Mg-HCO3	1.3	0.8	-5.5	-36				This study		
34	PN10	P	B	N. Pout	2008/06	39-81	30.4	7.2	710	92.2	19.4	23.1	1.2	54.3	25.7	5.9	1.7	308.5	2.1	26.3	0.19	0.11	Ca/Mg-HCO3	0.5	1.5	-5.4	-36				This study		
35	PN6	P	B	N. Pout	2008/06	38-60	29.9	7.3	808	112.5	23.4	19.2	0.8	38.7	23.2	5.0	2.1	431.0	3.5	26.1	0.54	0.81	Ca/Mg-HCO3	1.2	1.3	-5.6	-36				This study		
36	PN8	P	B	N. Pout	2008/06	42-62	30.8	7.0	770	103.3	21.8	24.6	1.3	53.3	35.6	7.3	2.3	356.3	2.2	34.6	0.11	-0.04	Ca/Mg-HCO3	0.4	1.5	-5.5	-37	7.1	0.1	-8.8	This study		14,500
37	Baity.D	P	B	East	2008/06	176-201	34.2	7.2	1268	89.5	64.2	69.7	10.0	193.8	182.9	<0.3	1.4	220.2	1.3	21.9	0.10	0.43	Ca/Na-Cl	b.d.	0.8	-5.0	-31				This study		
38	Kissane	P	B	East	2008/06	78-150	29.2	7.5	719	91.1	24.7	21.2	1.0	39.6	26.8	13.0	2.2	346.7	2.1	34.2	0.60	0.93	Ca/Mg-HCO3	0.6	0.9	-5.6	-36				This study		
39	Ngolfagning	P	B	East	2008/06	96-142	30.6	7.2	791	122.5	19.3	18.3	0.7	34.8	12.2	10.0	5.2	440.5	1.4	45.5	0.50	0.59	Ca/Mg-HCO3	<0.4	0.7	-5.7	-38				This study		
40	Samane	P	B	East	2008/06	18-44	31.8	6.8	1077	97.4	42.8	64.3	1.7	128.1	17.0	<0.3	3.4	455.2	2.4	75.1	0.01	0.08	Ca/Mg-HCO3	0.5	0.9	-5.5	-34				This study		
41	Tasset	P	B	East	2008/06	74-82	30.9	7.0	693	88.9	22.8	19.3	0.9	53.2	5.4	21.0	2.2	325.9	1.9	40.9	0.02	-0.13	Ca/Mg-HCO3	1.6	0.8	-5.6	-37				This study		
42	Diass	M	B	Diass	2008/06	80-110	31.1	7.0	182	16.3	2.4	11.4	1.8	23.1	1.3	28.2	0.0	23.2	2.3	15.0	-1.60	-3.70	Ca/Na-Cl	0.3	0.9	-5.9	-38				This study		
43	Guereo	M	B	Diass	2008/06	123-155	30.5	7.4	833	89.2	17.1	57.6	7.6	53.9	85.9	1.9	2.7	324.8	1.5	42.2	0.40	0.51	Ca/Mg-HCO3	<0.3	0.9	-4.7	-30				This study		
44	Ndayane	M	B	Diass	2008/06	184-217	32.1	6.7	714	110.4	15.1	19.1	3.4	18.3	62.2	<0.3	2.7	365.1	1.9	45.6	-0.20	-0.77	Ca/Mg-HCO3	<0.2	0.6	-5.1	-32				This study		
45	Ngekokh	M	B	Mbour	2008/06	172-184	27.6	6.9	743	81.5	14.3	24.4	4.9	19.8	40.6	<0.3	1.7	307.4	2.2	20.4	-0.20	-0.72	Ca/Mg-HCO3	<0.2	0.7	-4.9	-29				This study		
46	Ngekokh bis	M	B	Mbour	2008/06	-	31.0	7.1	736	93.3	14.1	23.6	5.1	19.8	41.3	<0.3	2.2	346.7	2.1	34.7	0.20	-0.04	Ca/Mg-HCO3	0.2	0.7	-4.9	-30				This study		
47	PK3	M	B	Diass	2008/06	192-259	30.9	6.7	524	94.1	5.3	7.3	2.2	14.8	7.5	<0.3	1.4	306.7	2.5	21.8	-0.20	-1.29	Ca/Mg-HCO3	0.1	0.9	-5.7	-38	41.8	0.1	-9.8	This study		730
48	PK5	M	B	Diass	2008/06	219-294	32.8	7.0	601	86.8	8.0	14.5	4.1	17.3	16.6	<0.3	2.1	305.3	1.7	41.0	0.10	-0.41	Ca/Mg-HCO3	<0.1	0.8	-5.6	-36				This study		
49	PS7	M	B	Diass	2008/06	210-260	32.8	6.6	625	117.0	6.9	8.7	2.8	12.1	6.0	<0.3	2.2	395.4	2.7	18.8	-0.10	-0.98	Ca/Mg-HCO3	b.d.	0.9	-5.7	-36				This study		
50	Sindia	M	B	Diass	2008/06	145-165	31.5	6.2	640	97.6	14.7	16.7	2.4	14.1	23.8	<0.3	1.9	377.7	2.9	25.8	-0.70	-1.74	Ca/Mg-HCO3	<0.6	0.8	-5.6	-35				This study		
51	Thicky	M	B	Diass	2008/06	78-121	31.0	7.5	385	61.7	4.4	9.0	1.1	15.9	20.6	15.5	1.2	153.6	0.8	35.0	0.10	-0.45	Ca/Mg-HCO3	0.5	0.8	-5.6	-38				This study		
52	F1 Saly	M	B	Mbour	2008/06	173-205	32.7	6.7	783	95.3	18.3	45.7	7.1	38.3	61.9	<0.3	1.9	380.1	2.9	15.7	-0.20	-0.64	Ca/Mg-HCO3	<0.3	0.8	-4.6	-27				This study		
53	F1bis Mbour	M	B	Mbour	2008/06	192-227	33.4	6.7	2990	54.3	58.5	472.3	21.5	764.6	118.2	8.1	3.2	312.8	1.2	26.9	-0.60	-0.76	Na-Cl	<0.1	1.0	-5.2	-34				This study		
54	F2 Saly	M	B	Mbour	2008/06	258-298	34.4	7.1	620	41.6	16.2	63.9	9.0	46.9	21.9	<0.3	2.1	278.6	1.4	22.8	-0.20	-0.37	Ca/Mg-HCO3	<0.6	0.8	-5.4	-36				This study		
55	F3 Mbour	M	B	Mbour	2008/06	107-191	32.1	7.1	931	51.1	20.4	112.2	8.3	123.3	36.8	<0.3	3.4	323.4	1.2	41.9	-0.10	-0.20	Na-HCO3	<0.4	0.9	-4.9	-31				This study		
56	F6 Mbour	M	B	Mbour	2008/06	80-175	32.2	7.0	1602	57.6	23.9	233.5	7.9	377.5	26.6	<0.3	2.0	258.1	1.3	14.8	-0.30	-0.58	Na-Cl	<0.7	1.1	-4.8	-31				This study		
57	F7 Mbour	M	B	Mbour	2008/06	100-192	31.8	6.7	620	53.1	17.9	43.4	6.1	41.9	33.0	<0.3	2.0	262.9	1.3	21.2	-0.50	-1.04	Ca/Mg-HCO3	0.0	0.8	-5.0	-33				This study		
58	F8 Mbour	M	B	Mbour	2008/06	101-195	32.6	6.7	608	49.0	16.1	44.9	6.2	47.5	25.6	<0.3	1.5	240.8	1.5	15.0	-0.60	-1.15	Ca/Mg-HCO3	<0.5	0.9	-5.0	-32				This study		
59	F9 Mbour	M	B	Mbour	2008/06	100-195	31.3	7.1	581	56.5	17.8	43.6	7.2	42.4	33.4	<0.3	1.9	270.4	1.5	13.8	-0.20	-0.38	Ca/Mg-HCO3	<0.2	0.8	-4.9	-31	48.6	0.1	-6.4	This study		actual
60	K. Balla	M	B	Mbour	2008/06	115-135	31.5	7.3	957	51.3	17.2	118.7	7.3	146.2	26.1	<0.3	2.3	292.7	1.4	12.1	0.01	-0.03	Na-HCO3	0.1	0.9	-4.5	-28				This study		
61	Takhoum	M	B	Mbour	2008/06	188-195	31.1	7.6	1517	93.9	28.6	133.3	12.3	329.9	17.6	<0.3	1.1	217.2	1.6	51.0	0.50	0.86	Ca/Na-Cl	b.d.	0.8	-5.0	-30				This study		
62	PS4	M	B	S. Pout	2008/06	260-320	31.5	6.9	558	94.8	6.1	6.4	1.8	11.0	7.4	<0.3	1.1	313.5	3.5	15.9	-0.02	-0.80	Ca/Mg-HCO3	<0.3	0.8	-5.8	-37				This study		
63	PS6	M	B	S. Pout	2008/06	252-305	32.3	7.1	615	94.3	7.9	7.9	2.9	12.2	7.3	<0.3	1.2	325.6	3.5	15.3	0.20	-0.20	Ca/Mg-HCO3	0.7	1.1	-5.6	-37				This study		
64	PN1	M	B	N. Pout	2008/06	-	33.0	7.0	658	103.0	8.9	10.1	4.3	10.4	7.6	<0.3	2.0	375.1	2.7	25.9	0.20	-0.27	Ca/Mg-HCO3	<0.4	0.9	-5.5	-36				This study		
65	PN11	M	B	N. Pout	2008/06	276-336	34.3	7.5	702	53.2	11.1	27.5	7.2	31.3	24.0	<0.3	1.3	218.0	1.4	15.2	0.20	0.24	Ca/Mg-HCO3	0.2	1.5	-4.4	-27				This study		
66	PN12	M	B	N. Pout	2008/06	275-335	33.6	7.4	688	78.3	12.5	32.5	7.4	40.3	26.5	<0.3	1.8	301.1	1.9	18.7	0.40	0.40	Ca/Mg-HCO3	0.5	1.5	-4.7	-30				This study		
67	PN2 bis	M	B	N. Pout	2008/06	-	33.7	7.1	668	93.1	8.5	21.6	3.5	17.9	12.2	<0.3	1.6	367.4	3.2	13.9	0.20	-0.15	Ca/Mg-HCO3	<0.1	0.7	-5.2	-33				This study		
68	PN3	M	B	N. Pout	2008/06	317-372	32.9	7.3	702	95.5	9.6	28.3	6.5	22.5	27.9	<0.3	2.6	359.3	2.0	38.9	0.40	0.24	Ca/Mg-HCO3	1.7	1.5	-4.8	-30				This study		
69	PN4	M	B	N. Pout	2008/06	279-331	32.7	7.3	683	96.3	9.8	14.2	4.6	13.8	11.5	<0.3	1.3	358.2	3.7	13.8	0.40	0.27	Ca/Mg-HCO3	0.5	1.4	-5.1	-31				This study		
70	PN5	M	B	N. Pout	2008/06	264-320	32.6	6.8	690	117.4	10.2	15.2	4.2	15.0	12.1	<0.3	1.9	432.6	3.8	15.4	0.10	-0.38	Ca/Mg-HCO3	0.4	1.4	-4.9	-31				This study		
71	PN7	M	B	N. Pout	2008/06	216-331	32.4	7.2	707	74.5	14.4	21.3	6.0	25.3	22.9	<0.3	1.5	295.6	2.3	13.7	0.10	-0.05	Ca/Mg-HCO3	1.2	1.5	-4.7	-28				This study		
72	PN9	M	B	N. Pout	2008/06	268-348	33.2	7.0	703	99.1	12.1	25.4	6.9	28.6	22.5	<0.3	1.4	370.2	3.8	15.2	0.20	-0.16	Ca/Mg-HCO3	1.5	1.3	-4.4	-27				This study		
73	Sandiara	M	B	East	2008/06	168-191	33.2	7.8	2300	22.2	11.4	442.9	12.5	537.7	46.2	<0.3	2.6	332.4	1.6	54.0	0.14	0.42	Na-Cl	b.d.	1.0	-4.3	-28				This study		
74	K.Moussa	M	B	Sebi	2008/06	110-150	29.6	6.4	301	31.2	5.2	15.7	4.4	31.0	13.4	6.3	0.1	86.4	2.9	18.8	-1.50	-3.34	Ca/Mg-HCO3	<0.1	0.8	-5.9	-38				This study		
75	Thiès F2	M	B	East	2008/06	559-592	38.2	7.0	642	102.2	8.3	21.1	8.5	21.6	18.6	<0.3	1.9	370.5	2.8	28.1	0.30	-0.04	Ca/Mg-HCO3	0.1	1.0	-4.5	-26				This study		
	Pop 1	R	S	Diass	2008/07/1-15			7.5	160	23.8	1.8	12.9	2.8	19.4	14.2	3.4	0.1	69.8	1.7	1.0			Ca/Mg-HCO3	2.9	0.8	-3.2	-18				This study		
	Pop 2	R	S	Diass	2008/07/16-31			7.2	63	8.4	1.1	5.7	0.6	6.5	3.6	0.7	0.0	34.9	1.4	0.9			Ca/Mg-HCO3	1.9	0.7	-5.3	-31				This study		
	Pop 3	R	S	Diass	2008/08/1-15			7.0	61	8.4	0.7	4.8	0.5	5.7	3.3	2.3	0.0	30.1	2.0	0.7			Ca/Mg-HCO3	2.0	0.7	-5.5	-33				This study		
	Pop 4	R	S	Diass	2008/08/16-31			6.6	51	5.2	0.7	4.1	0.4	5.8	3.7	0.9	0.0	20.3	3.3	0.6			Ca/Mg-HCO3	2.7	0.7	-6.9	-46				This study		
	Pop 5	R	S	Diass	2008/09/1-15			6.7	48	3.9	0.6	4.9	0.5	6.5	2.3	0.5	0.0	18.4	2.5	0.4			Ca/Mg-HCO3	1.7	0.7	-5.4	-32				This study		
76	Pop 6	R	S	Diass	2008/09/16-30			6.5	50	4.6	0.9	4.6	0.7	9.3	1.9	1.3	0.0	12.9	3.2	0.2			Ca/Na-Cl	3.4	0.8	-6.6	-42				This study		
	Mbour 1	R	S	Mbour	2008/07/1-15			7.4	47	6.6	0.7	3.5	0.5	6.2	3.5	4.4	0.0	12.4	0.3	0.0			Ca/Na-Cl	3.9	1.1	-5.3	-30				This study		
	Mbour 2	R	S	Mbour	2008/07/16-31			7.1	31	3.6	0.5	2.6	0.3	4.0	1.5	0.4	0.0	11.6	0.7	0.0			Ca/Mg-HCO3	1.7	0.7	-2.6	-12				This study		
	Mbour 3	R	S	Mbour	2008/08/1-15			6.5	16	1.6	0.1	1.4	0.3	2.1	1.3	1.0	0.0	3.8	0.9	0.1			Ca/Na-Cl	3.3	0.7	-7.2	-47				This study		
	Mbour 4	R	S	Mbour	2008/08/16-31			6.2	21	2.7	0.3	1.9	0.3	2.9	1.2	2.5	0.0	4.8	1.9	0.0			Ca/Na-Cl	3.9	0.8	-7.1	-45				This study		
	Mbour 5	R	S	Mbour	2008/09/1-15			5.6	20	1.9	0.3	1.9	0.3	2.9	1.1	2.9	0.0	1.5	0.4	0.9			Ca/Na-Cl	2.2	0.7	-6.3	-42				This study		
77	Mbour 6	R	S	Mbour	2008/09/16-30			5.9	25	3.8	0.3	1.2	0.5	1.4	1.0	7.1	0.0	6.7	4.5	0.4			Ca/Mg-HCO3	3.4	0.7	-6.1	-33				This study		
	Kirene 1	R	S	Mbour	2008/07/1-15			7.7	205	38.3	0.6	5.7	2.1	8.5	22.4	16.8	0.2	80.0	1.1	3.8			Ca/Mg-HCO3	3.1	0.7	-3.7	-20				This study		
	Kirene 2	R	S	Mbour	2008/07/16-31			7.5	108	22.5	0.6	2.5	0.7	3.8	7.6	3.2	0.1	63.8	1.6	2.0			Ca/Mg-HCO3	1.9	0.7	-5.8	-33				This study		
	Kirene 3	R	S	Mbour	2008/08/1-15			7.3	91	17.6	0.3	1.3	0.8	2.7	5.9	1.7	0.1	47.6	1.5	1.0			Ca/Mg-HCO3	2.2	0.7	-6.1	-37				This study		
78	Kirene 4	R	S	Mbour	2008/08/16-31			7.2	80	13.1	0.4	1.3	0.7	1.8	3.5	0.8	0.1	46.3	1.9	0.5			Ca/Mg-HCO3	3.2	0.7	-6.4	-45				This study		
	Pout 1	R	S	Diass	2008/07/1-15			7.2	85	6.7	0.9	4.1	3.1	6.9	5.3	4.7	0.0	19.5	1.0	0.0			Ca/Mg-HCO3	4.2	0.8	-3.8	-21				This study		
	Pout 2	R	S	Diass	2008/07/16-31			7.1	76	6.9	0.5	2.5	1.7	4.6	4.3	10.6	0.0	16.3	0.8	0.0			Ca/Mg-HCO3	2.7	0.7	-5.1	-30				This study		
	Pout 3	R	S	Diass	2008/08/1-15			6.8	87	11.5	0.6	3.0	3.1	4.8	4.5	29.2	0.0	10.6	1.1	0.0			Ca/Na-Cl	2.5	0.7	-4.7	-27				This study		
	Pout 4	R	S	Diass	2008/08/16-31			6.6	30	3.5	0.2	0.8	0.7	1.4	1.5	0.3	0.0	12.4	2.0	0.0			Ca/Mg-HCO3	3.0	0.7	-6.2	-36				This study		
	Pout 5	R	S	Diass	2008/09/1-15			6.5	17	1.6	0.2	0.7	0.5	1.1	0.8	0.5	0.0	6.3	1.6	0.2			Ca/Mg-HCO3	2.2	0.7	-5.7	-37				This study		
79	Pout 6	R	S	Diass	2008/09/16-30			6.5	31	4.1	0.2	0.5	0.7	1.3	1.7	6.8	0.0	5.9	1.4	0.0			Ca/Mg-HCO3	4.8	0.8	-4.0	-22				This study		
	Thies 1	R	S	East	2008/07/1-15			7.3	157	13.4	1.1	18.1	5.3	12.1	15.6	6.0	0.2	63.5	1.3	0.9			Na-HCO3	3.4	0.7	-3.9	-23				This study		
	Thies 2	R	S	East	2008/07/16-31			7.8	191	30.5	1.3	19.2	6.9	13.8	17.3	3.5	0.5	121.1	1.4	0.8			Ca/Mg-HCO3	2.3	0.7	-3.2	-21				This study		
	Thies 3	R	S	East	2008/08/16-31			7.4	79	19.3	0.4	2.7	0.3	2.0	2.3	2.2	0.1	66.0	1.8	0.0			Ca/Mg-HCO3	2.4	0.7	-4.6	-28				This study		
	Thies 4	R	S	East	2008/09/1-15			7.1	78	14.9	0.9	3.1	1.0	2.5	3.3	5.7	0.1	55.9	2.2	1.1			Ca/Mg-HCO3	1.3	0.7	-4.6	-31				This study		
80	Thies 5	R	S	East	2008/09/16-30			7.4	81	15.5	0.8	4.0	0.9	4.1	3.7	3.5	0.1	56.8	1.6	0.6			Ca/Mg-HCO3	1.3	0.7	-4.8	-30				This study		
	Yenn 1	R	S	Diass	2008/07/1-15			7.7	361	40.0	2.9	41.9	12.0	40.7	25.3	13.2	0.5	134.6	1.8	4.5			Ca/Mg-HCO3	3.1	0.7	-3.9	-20				This study		
	Yenn 2	R	S	Diass	2008/07/16-31			7.4	218	24.7	2.9	24.7	4.4	27.4	9.8	3.2	0.4	89.2	2.9	1.9			Ca/Mg-HCO3	1.4	0.7	-5.2	-30				This study		
	Yenn 3	R	S	Diass	2008/08/1-15			6.9	100	11.5	1.3	9.2	1.7	11.4	4.2	4.7	0.0	36.6	2.8	1.2			Ca/Mg-HCO3	2.4	0.7	-6.9	-42				This study		
	Yenn 4	R	S	Diass	2008/08/16-31			7.4	135	13.6	1.8	15.5	1.8	15.6	5.4	1.7	0.1	60.7	1.5	1.5			Ca/Mg-HCO3	3.5	0.7	-6.0	-40				This study		
	Yenn 5	R	S	Diass	2008/09/1-15			7.6	164	4.8	1.2	20.7	7.1	19.0	5.6	0.5	0.2	74.5	1.4	0.6			Na-HCO3	1.3	0.7	-5.2	-31				This study		
81	Yenn 6	R	S	Diass	2008/09/16-30			7.4	74	6.4	0.8	9.9	0.9	7.6	2.4	1.4	0.0	31.5	1.0	0.8			Na-HCO3	2.2	0.7	-6.4	-43				This study		
	Kirene maraicher	M	B	Diass	1971/06/26	129-170		6.7										79.3						2.2		-5.9		70.8		-16.7	IAEA, 1972	3,000	1,800
	Kirène Maraicher	M	B	Diass	1982/06/22	129-170	31.0	5.8										488.0						8.4		-5.6	-34	65.7		-16.7	Faye, 1983	3,500	1,500
	kirene P11	M	B	Diass	1995/05/01	139-147	29.0	6.6										268.4						<0.1		-6.0	-36	66.4		-17.2	RAF, 1998		2,500
	Ndayane	M	B	Diass	1995/05/01	184-217	33.4	6.1										362.3						<0.3				28.6		-15.1	RAF, 1998		7,500
	Ndayane	M	B	Diass	1982/04/08	195 -208	32.6	6.9										373.3						11.4		-5.2	-20	29.8	0.8	-13.0	Faye, 1983	7,950	6,200
	Ndayane	M	B	Diass		195 -208	32.5	8.9										384.9								-5.9	-33	29.8		-13.0	Travi, 1988	10,500	6,800
	Ngarigne	M	B	Diass	1982/04/08	206-214	29.3	7.3										294.0						15.2		-5.3	-32	36.8		-12.8	Faye, 1983	6,050	4,600
	SE31M	M	B	Diass	1995/06/10		29.5	7.3										384.9										57.2	1.3	-9.9	Travi, 1988	6,000	actual
	Gandigal	M	B	Mbour	1982/04/08		32.0	6.8										337.9						7.7				12.2		-12.2	Faye, 1983	14,600	13,000
	Louly Bentegne	M	B	Mbour	1982/04/08		31.5	6.8										371.5								-4.9	-28	0.1	0.3	-12.7	Faye, 1983		
	Mbour	M	B	Mbour	1969/04/03			7.5										144.0						3.8		-5.2	-34	1.7		-9.3	IAEA, 1972	28,500	27,000
	Sali F1	M	B	Mbour	1982/06/22	173-205	33.2	6.9										295.2						16.6			-34	2.8	0.3	-10.0	Faye, 1983	25,300	23,000
	Somone F	M	B	Mbour	1995/05/01		31.6	6.3										392.3						0.4		-5.1	-28	8.6		-12.1	RAF, 1998		15,500
	Pout S6	M	B	S. Pout	1982/04/08	149 - 322	32.5	6.7										287.9						19.3		-6.0		37.8		-14.5	Faye, 1983		5,300
	Pout S6	M	B	S. Pout	1971/05/22	149 - 322		7.3										317.2						3.0				39.3		-15.4	IAEA, 1972	8,000	7,000
	Mekhe	M	B	East	1969/03/27																			0.4		-4.8	-30	0.7		-1.2	IAEA, 1972		18,500
	P7 K.Lemou	M	B	East	1970/10/04			7.8										170.8						0.8		-5.3		1.4		-4.6	IAEA, 1972	20,500	23,000
	Taiba 1	M	B	East	1969/03/26			7.0										85.4						1.0		-4.8	-24	1.6		-5.4	IAEA, 1972	18,500	23,000
	Thies1	M	B	East	1969/03/27			6.7										112.8						1.2		-4.4	-27	8.5		-11.8	IAEA, 1972	16,500	15,500
	Thies3	M	B	East	1969/03/27			7.0										192.2						0.1		-4.6	-29	1.6		-9.5	IAEA, 1972	28,500	28,000
	Tivaounane2	M	B	East	1969/03/26			7.0										91.5						0.5		-4.7	-27	2.2		-6.4	IAEA, 1972	19,500	22,000
	Pout F1	P	B	S. Pout	1969/03/27	41-46		6.5										201.9						2.8		-5.9	-39	51.5		-11.8	IAEA, 1972	500	800
	Pout F1	P	B	S. Pout	1972/01/13	41-46																		1.8		-5.8		56.2		-11.5	IAEA, 1972		actual
	PS3	P	B	S. Pout	1995/05/01		32.4	6.7										416.0						1.2		-6.4	-36	49.2		-12.1	RAF, 1998		1,200
	Sebi F1	P	B	Sebi	1969/04/03	24-58		7.2										259.9						0.3		-5.6	-34	36.4		-10.1	IAEA, 1972	3,500	2,300
	Sébi F3	P	B	Sebi	1995/05/01	65-82	29.9	7.1										347.6						0.6		-5.8	-36	36.9		-10.7	RAF, 1998		2,600
	Tanma P4	P	B	Sebi	1972/01/14	169 - 173		7.4										192.2						0.8		-5.1		4.5		-7.5	IAEA, 1972	17,500	17,000
	Thieudeum S3	P	B	Sebi	1971/03/18	100-104		7.4										247.1						2.9		-5.6		10.7		-8.3	IAEA, 1972	12,000	11,000
	Tasset P12	P	B	East	1971/05/17	46-112		7.6										335.5						15.4		-5.8		52.8		-12.6	IAEA, 1972	3,500	1,850

736 Vulnerability problems with groundwater resources in Africa

737

738 Over-exploitation of heterogeneous Dias aquifer system in Dakar region (Senegal)

739

740 Environmental isotopes as a unique tool to understand hydrodynamic and geochemical processes

741

742 Estimation of the recharge origin, water geochemistry and water types

743

744 Mixture processes of old and young water components

745